

# Sentiment-Driven Speculation in Financial Markets with Heterogeneous Beliefs: a Machine Learning approach \*

Tommaso Di Francesco  
t.difrancesco@uva.nl  
University of Amsterdam  
Ca' Foscari University of Venice

Cars Hommes  
University of Amsterdam  
Bank of Canada  
Tinbergen Institute

July 16, 2024

MOST RECENT VERSION [HERE](#)

## Abstract

We study an heterogeneous asset pricing model in which different classes of investors coexist and evolve, switching among strategies over time according to a fitness measure. In the presence of boundedly rational agents, with biased forecasts and trend following rules, we study the effect of two types of speculation: one based on fundamentalist and the other on rational expectations. While the first is only based on knowledge of the asset underlying dynamics, the second takes also into account the behavior of other investors. We bring the model to data by estimating it on the Bitcoin Market with two contributions. First, we construct the Bitcoin Twitter Sentiment Index (BiTSI) to proxy a time varying bias. Second, we propose a new method based on a Neural Network, for the estimation of the resulting heterogeneous agent model with rational speculators. We show that the switching finds support in the data and that while fundamentalist speculation amplifies volatility, rational speculation has a stabilizing effect on the market.

**Keywords:** *Asset Pricing; Heuristic Switching Model; Machine Learning.*

**JEL Classification:** *C63; D84; E32; E44; G12.*

---

\*This work has received funding from the European Union's Horizon 2020 research and innovation programme under the Marie Skłodowska-Curie grant agreement No 956107, "Economic Policy in Complex Environments (EPOC)". We thank Paolo Pellizzari, Alexandre Carrier, Andrea Tilton and Ekaterina Ugulava, as well as participants to the CeNDEF 2022 Seminar, the CEF 2023 Conference, the WEHIA 2023 and the 1st EPOC Jamboree in Barcelona for helpful comments and suggestions.

# 1 Introduction

Expectations play a crucial role in economics. Aggregate variables depend on the interaction and decisions of multiple individuals. Since these decisions depend on how agents expect the future to evolve, the way in which expectations are formed bears an effect on the aggregate variables themselves. Financial markets are a prime example of this *expectation feedback* since the price of an asset includes expectations regarding its performance, or its discounted cash flow, in the future. Classical asset pricing models usually assume agents with rational expectations (RE) a là [Muth \(1961\)](#). The RE hypothesis assumes that agents form expectations which are model consistent and based on all available information. Moreover, classical models assume a representative agent. While idiosyncratic errors across agents are permitted, on average the economy acts as if populated by a representative rational agent. If the RE hypothesis was true then the price of any financial asset should be equal to its *fundamental value*, the expected present value of dividends. The literature has long observed that this is not true for many assets, but one cannot easily disentangle the role of expectations from the one of the discount factor<sup>1</sup>.

In recent years however, we have had the emergence of an asset class, *cryptocurrencies* with no fundamental value. In particular, Bitcoin, the first and most known cryptocurrency is the 9th asset for market capitalization with a value of 1.3 trillion dollars as of April 2024. Since Bitcoin does not and will never pay dividends, there is no discount factor which can explain a non zero price. Among the possible explanations that can still maintain the RE hypothesis, two are the most prominent. The first one is that of Bitcoin as a *rational bubble*, for which all investors agree that the price will indefinitely grow at a rate higher than the risk-free rate. The second is that although there are no dividends associated with it, Bitcoin provides investors with some *convenience yield*. Tax evasion and purchasing of illegal goods are classical examples. Both explanations have drawbacks. The first because any transversality condition would make the rational bubble collapse as long as agents are rational. The second because it would imply a convenience yield almost as volatile as the Bitcoin price.

In this paper we propose a different explanation: *sentiment driven speculation*. We relax the RE assumption in one dimension, namely homogeneity and allow for heterogeneous investors in the market. As [Shalen \(1993\)](#) notes “*it is well understood that speculative trade in financial markets depends on divergent beliefs*”. Papers like [De Long et al. \(1990\)](#) introduce the concept of *noise traders*, a group of investors systematically acting on some signal uncorrelated with an asset fundamental. In a similar spirit, [Harris and Raviv \(1993\)](#) and [Hong and Stein \(2003\)](#) study the effect on the market of differences of opinion among investors. A common theme of all these papers is that the different beliefs are exogenously determined. [Brock and Hommes \(1998\)](#) is a noticeable attempt to endogenize the divergence of beliefs by proposing an Heuristic Switching Model (HSM). Building on this work, our Bitcoin model considers a market with bias investors and trend chasers whose fractions evolve endogenously according to their realized profits. Bias investors believe that the

---

<sup>1</sup>See for example [Adam and Nagel \(2023\)](#).

fundamental value of Bitcoin is some positive value. Since this belief is not dictated by any financial reason, we also refer to them as *sentiment followers*. Trend chasers add a short-term demand, driven by momentum. Given the presence of non rational behaviors among investors, one would expect speculation to be possible in the market. Therefore, we study two types of speculation, one associated with fundamentalist and one with rational expectations. It is important to notice that the two do not coincide because of the presence of heterogeneous agents. Perfect rationality requires knowledge not only of the asset fundamental but also of the strategies adopted by other individuals. It coincides with *perfect foresight* in a deterministic setting. To solve for RE we rely on the Extended Path (EP) method of [Fair and Taylor \(1983\)](#). We then bring the model to the data introducing two contributions. First, we propose to capture the bias of agents in the market by constructing an index based on textual data from Twitter. Using a dataset of more than ten million tweets containing the word “Bitcoin” we construct the Bitcoin Twitter Sentiment Index (BiTSI) through sentiment analysis in the form of the Valence Aware Dictionary and sEntiment Reasoner (VADER). Second, while there are multiple estimations of HSM in the literature, none of them, to the best of our knowledge, include rational investors. One of the reasons is that in order to estimate the model according to the [Fair and Taylor \(1983\)](#) method, one has to first solve for RE using the EP for each combination of the parameters of interest. As the parameter space grows exponentially with every additional parameter, this method suffers from the *curse of dimensionality*. We propose to tackle this issue with a Machine Learning model. Specifically, we show that it is possible to approximate RE with a Neural Network (NN) model. In practice, we re-parameterize the problem such that we only need to estimate the rational expectations vector once. After obtaining the vector, estimating the model can be done by normal Non-Linear Least Squares.

The rest of the paper is structured as follows: section [1.1](#) discusses some related literature, section [2](#) introduces the HSM, section [3](#) introduces the BiTSI index, section [4](#) introduces our method to estimate the non-linear RE model and shows its effectiveness on simulated data, section [5](#) estimates the models on real data, section [6](#) concludes.

## 1.1 Related Literature

On the theoretical side this paper relates to the literature on HSM, started by the [Brock and Hommes \(1997\)](#) paper. Their seminar paper focuses on a Cobweb model. Since the agents need to make a one period ahead prediction, they are able to analyze a model including also RE. In financial markets the prediction is a two-step ahead one which makes the analysis of the model with RE non trivial. Also for this reason in [Brock and Hommes \(1998\)](#) after analyzing the steady states for the model with perfect foresight, the authors replace this heuristic with fundamentalist traders. The interplay among fundamentalist, chartists and bias agents has been studied extensively both in discrete [Hommes, Huang and Wang \(2005\)](#) and continuous [He and Li \(2012\)](#) time and the reader can refer to [Hommes \(2021\)](#) for an extensive survey of the literature. A notable exception is [Boehl and Hommes \(2021\)](#) in which the authors develop a new algorithm to compute perfect foresight in an HSM. With

respect to their paper we use a different solution procedure to obtain the perfect foresight solution and provide a method to estimate the resulting non-linear heterogeneous agent rational model. Moreover while in our case the non-linearity is given by heterogeneity, our method is general and can be applied to any type of non-linear model with RE. This is important since while some papers like Fisher, Holly and Hallett (1986) and Armstrong et al. (1998) have improved the original Fair and Taylor (1983) method in terms of robustness and efficiency, their focus has been only on solving for RE and not on estimation.

This method allows us to contribute to the literature on the empirical validity of HSM, by estimating for the first time a model with the RE heuristic. In this area, most papers relied on Non-Linear Least Squares to estimate a model with mean-reverter (fundamentalist) and chartists (trend-followers) on the S&P 500 Boswijk, Hommes and Manzan (2007) and Chiarella et al. (2014), the option market Frijns, Lehnert and Zwinkels (2010), the gold market Baur and Glover (2014), the European Credit Default Swap market Chiarella, He and Zwinkels (2014), the housing market Bolt et al. (2019), US inflation dynamics Cornea-Madeira, Hommes and Massaro (2019) or a comparison across asset classes ter Ellen, Hommes and Zwinkels (2021). Lof (2015) also focuses on the S&P 500 but introduces a third type of agents labeled *rational* which in our setting would be short-term fundamentalists and hence different from RE traders. Finally some papers like Franke and Westerhoff (2012) and Schmitt (2021) rely on the Simulated Method of Moments to estimate a model with fundamentalists and chartists.

Another difference with this literature is that we estimate a model including bias investors. For this we bridge the HSM estimation literature with the one focusing on the role of sentiment in the Bitcoin Market which we use as a proxy of time varying bias. The Bitcoin market exhibits a lesser degree of efficiency compared to other financial markets and is more prone to speculative bubbles and other market inefficiencies, potentially leading to substantial investor losses and presenting numerous arbitrage opportunities, as evidenced in studies like Cheah and Fry (2015), Urquhart (2016) and Makarov and Schoar (2020). In this setting multiple papers have focused on the effect of sentiment measured on the website StockTwits Chen and Hafner (2019), Guégan and Renault (2021), on Google Trends Urquhart (2018), Aalborg, Molnár and de Vries (2019), Baig, Blau and Sabah (2019), Liu and Tsyvinski (2020), X J.Parra-Moyano et al. (2024), the Cryptocurrency Forum Sentiment Gurdgiev and O'Loughlin (2020) or the Fear and Greed Index Bourghelle, Jawadi and Rozin (2022). However, while this literature is empirical and relies on a reduced form estimation, we estimate a structural model which offers a clear mechanism on how sentiment and switching among different strategies can explain the highly volatile Bitcoin market environment.

## 2 The model

The economy is populated by  $I$  investors with  $J$  different beliefs to be specified below. Time is discrete. We assume that the fundamental value of the asset is equal to 0. This

implies that any positive price can be seen as price deviation from the fundamental value. The equilibrium price of the asset is derived from the maximization problem of mean-variance maximizers agents and given by

$$Rp_t = \sum_{j=1}^J n_{j,t} \mathbb{F}_{j,t}(p_{t+1}) + \varepsilon_t, \quad (1)$$

where  $\mathbb{F}_{j,t}(p_{t+1})$  is the subjective forecast implied by belief  $j$  and  $R = 1 + r$  is the gross risk-free rate. Timing is important and we assume that the current equilibrium price  $p_t$  is not realized and therefore not available to the agents when forming their beliefs. In other words they are making a two period ahead forecast. Equation (1) simply states that the current price is a weighted average of the different  $J$  beliefs, weighted by the fraction of the population  $n_{j,t}$  that embraces the belief at time  $t$ .  $\varepsilon_t$  is normal, identical and independently distributed noise. Fractions are updated every period according to a fitness measure that is public knowledge and is given by past returns in excess of the risk-free rate

$$\pi_{j,t} = (p_t - Rp_{t-1}) (\mathbb{F}_{j,t-1}(p_t) - Rp_{t-1}). \quad (2)$$

The fraction of agents choosing strategy  $j$  is given by the multinomial logit model [Manski and McFadden \(1981\)](#)

$$n_{j,t} = \frac{e^{\beta \pi_{j,t-1}}}{\sum_{j=1}^J e^{\beta \pi_{j,t-1}}}. \quad (3)$$

The parameter  $\beta$  represents the intensity of choice. When  $\beta = 0$ , agents simply randomize in their predictor's choice, and fractions are constant at  $1/J$ . When  $\beta \rightarrow \infty$  agents immediately switch to the most profitable strategy, and all but the fraction associated with the best strategy are zero. Equations (1) and (3) jointly determine the full price and fractions evolution. A micro-foundation of the model is given in [Appendix A](#). It is important to notice that realized profits and forecast accuracy are not perfectly proportional. When an individual has a perfect forecast, their profits are guaranteed to be positive and given by  $(p_t - Rp_{t-1})^2$ . However for an individual with incorrect forecast to earn more than this quantity it is sufficient to be inaccurate in the "right direction". Consider the quantity  $(p_t - Rp_{t-1}) (\mathbb{F}_{j,t-1}(p_t) - p_t)$  which represents the numerator of the difference in realized profits obtained by a perfectly accurate individual, and a generic individual employing strategy  $j$ . For this quantity to be positive, thus consisting of more profits for the agent using the "incorrect forecast", it is sufficient that

$$\text{sgn}(p_t - Rp_{t-1}) \cdot \text{sgn}(\mathbb{F}_{j,t-1}(p_t) - p_t) = 1,$$

with  $\text{sgn}(x) = x/|x|$  is the sign function. The intuition is that the forecasting error has the same direction of the price change. The reason why even with a perfect forecast an individual does not purchase or sell unlimited quantities of the risky asset is the bound imposed by their risk aversion and the variance of the risky asset. Incorrect investors are overly optimistic or pessimistic, therefore purchasing or selling more than they should.

Sometimes, by chance, their overconfidence pays off.

## 2.1 Expectations

We assume that all forecasting strategies are given by a linear function of past and future prices and of a bias process.

$$\mathbb{F}_{j,t}(p_{t+1}) = h_{j,t}(\{p_{t-l}\}_{l=1}^L, \{\mathbb{E}_t(p_{t+j})\}_{j=0}^K, \{w_{t-l}\}_{l=1}^L).$$

with  $w_t$  being an observable i.i.d stochastic process independent of prices. The functional form allows for simple but typical beliefs supported by experimental evidence as in [Hommes et al. \(2005\)](#) or for more sophisticated ones. The formulation so far is general enough to accommodate for a multiplicity of strategies as in [Brock, Hommes and Wagener \(2005\)](#), but we will focus on 4 strategies that are representative of behaviors we expect to see in the market and are summarized below.

**Trend chasers.** Sometimes also referred to as chartists. They form their forecast by an analysis of past prices. We consider the simplest form given by

$$h_{j,t}(\{p_{t-l}\}_{l=1}^L, \{\mathbb{E}_t(p_{t+j})\}_{j=0}^K, \{w_{t-l}\}_{l=1}^L) = gp_{t-1}, \quad g > 0. \quad (4)$$

In forming their expectations they extrapolate from last period price deviation. The parameter  $g$  being greater than 0 implies that they expect positive price deviations to continue. The magnitude of  $g$  determines the degree of trend following with the case  $g > R = 1 + r$  usually referred to as *strong trend chasing*. The presence of this category of investors in the system is consistent with evidence provided by the literature about the existence of a momentum factor in stock markets, and originated by the seminal paper of [Jegadeesh and Titman \(1993\)](#).

**Pure bias.** This class of investors base their beliefs on some process which in the empirical part we will think of as *sentiment*, unrelated to the asset fundamentals or prices. Their forecast is

$$h_{j,t}(\{p_{t-l}\}_{l=1}^L, \{\mathbb{E}_t(p_{t+j})\}_{j=0}^K, \{w_{t-l}\}_{l=1}^L) = bw_{t-1}, \quad b > 0. \quad (5)$$

**Fundamentalists.** Investors of this type base their expectations on the fundamental value of the asset. They would be rational in a homogeneous rational world in the sense that if the market would be populated only by fundamentalists, then their forecast will be the correct one. They do however fail to take into consideration the presence of boundedly rational agents with different beliefs in the market. Recalling that the fundamental value in this setting is equal to 0 we have

$$h_{j,t}(\{p_{t-l}\}_{l=1}^L, \{\mathbb{E}_t(p_{t+j})\}_{j=0}^K, \{w_{t-l}\}_{l=1}^L) = 0. \quad (6)$$

**Rational expectations.** They are the more sophisticated investors having knowledge of the

underlying model regulating the asset price evolution and the composition of the market. Their forecast is the correct one and coincides with the one the modeler would obtain:

$$h_{j,t}(\{p_{t-l}\}_{l=1}^L, \{\mathbb{E}_t(p_{t+j})\}_{j=0}^K, \{w_{t-l}\}_{l=1}^L) = \mathbb{E}_t(p_{t+1}). \quad (7)$$

We now investigate the dynamics that can emerge from the interactions of these simple strategies. The first case we consider is a two type market.

## 2.2 Trend chasers vs pure bias

We take the first strategy to be trend chasing as in (4) and the second one to be pure bias (5). We start by considering deterministic simulations and assume that  $w_{t-1}$  is constantly equal to its expected value which we fix to 1 without loss of generality. We also keep the noise component  $\varepsilon$  fixed at its expected value of 0.

The full model is therefore given by the following two equations:

$$Rp_t = n_{1,t}gp_{t-1} + (1 - n_{1,t})b, \quad (8)$$

$$n_{1,t} = \{1 + \exp(\beta(p_{t-1} - Rp_{t-2})(b - gp_{t-3}))\}^{-1}. \quad (9)$$

We provide an analytical characterization of the steady states of the system, for extreme values of the intensity of choice parameter  $\beta$ .

**Lemma 1 (Steady States for the two type model)** *For  $\beta = 0$  the model has a unique and locally stable steady state  $p = \frac{b}{2R-g}$ . For  $\beta \rightarrow +\infty$  there are the following possibilities. If  $g = R$  then any  $0 < p \leq \frac{b}{R}$  is a steady state with all steady state  $0 < p < \frac{b}{R}$  being locally unstable and  $p = \frac{b}{R}$  being locally stable. If  $g > R$  there exists a unique steady state  $p = \frac{b}{R}$  which is locally stable. If  $g < R$  there are no (positive) steady states.*

*Proof.* See Appendix B.

The lemma shows that the even in the neoclassical limit in which agents immediately switch to the best performing strategy, pure bias agents are not pushed out of the market. Indeed the most interesting case is the one in which  $g > R$  and trend chasing is *strong*. In this situation the steady state is a positive deviation from the fundamental value, the magnitude of which depends on  $b$ . When  $\beta$  is strictly positive, the steady state equation can only be derived implicitly. We do this in Appendix C while below we use numerical simulations to highlight the global dynamics that this system may generate.

## 2.3 Numerical Simulations: $b = 1.0$ , $g = 1.3$ , $R = 1.01$

We fix all parameters but the intensity of choice  $\beta$ . We then study the global dynamics of the model. First, we report a Bifurcation diagram for increasing value of the intensity of choice parameter. For each value of  $\beta$  we simulate 10000 iterations of the system, and



then visualize the last 2000 price realisations, in order to eliminate the effect of initial conditions. In panel (a) of Figure 1 we can observe that the system has a stable steady state for values of the intensity of choice lower than approximately 6.725. After the parameter crosses this value, a bifurcation occurs. In order to characterize this bifurcation and the system dynamics after bifurcation, we use maximum lyapunov exponents<sup>2</sup> and a plot of the modulus of the system eigenvalues. The maximum lyapunov exponent is a convenient tool to detect chaos in dynamical system, which is associated with positive values of the exponent. As we can see in panel (b) of Figure 1 the exponent is negative for low values of  $\beta$  and becomes equal to 0 after the bifurcation. Therefore the system exhibits periodic and quasi periodic orbits, never producing chaos. In panel (c) we plot the modulus of the eigenvalue of the system, that we compute in section (B.4) of the appendix. We can see that for values of  $\beta \approx 6.725$  the two complex eigenvalues cross the unit circle. We conclude therefore that a Hopf bifurcation occurs. Finally in panel (d) we show the creation of stable invariant circles after the bifurcation, allowing us to classify the bifurcation as super-critical.

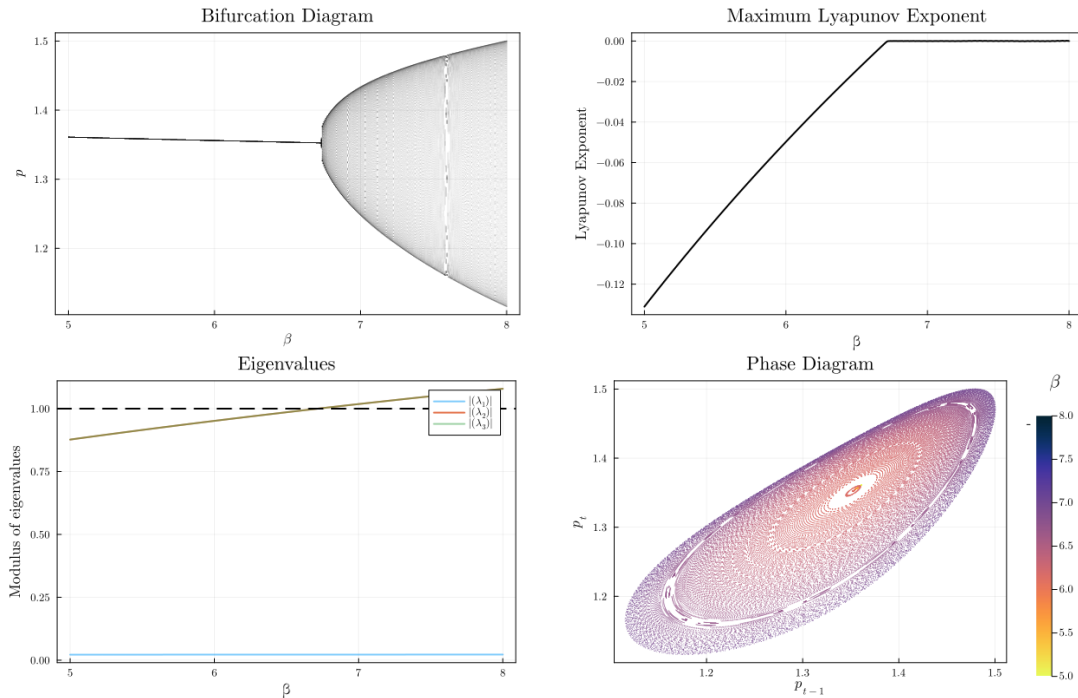


Figure 1: Numerical simulations for the two type system, other parameters are  $g = 1.3$ ,  $b = 1$ ,  $R = 1.01$ . A Hopf bifurcation occurs for  $\beta \approx 6.725$ , as the two complex eigenvalues have modulus  $|\lambda_2| = |\lambda_3| = 1$ . After the bifurcation periodic and quasi periodic orbits are created.

We then investigate the mechanism responsible for the orbit observed, by plotting the trajectory of the system and the fractions evolution for a value of the intensity of choice  $\beta = 7.0$ , in Figure 2. The bubble and burst behavior is caused by oscillating periods of

<sup>2</sup>The computation is an in-built function of the package Julia package DynamicalSystems.jl, that relies on the method by [Benettin et al. \(1980\)](#).



optimism and pessimism. Pure bias agents act in a way which is qualitatively similar to fundamentalists in the original [Brock and Hommes \(1998\)](#) paper, but their bias implies that the fluctuations are translated upward. The bubble is sustained by a growing population of trend chasers in the market. As long as the next period has a higher concentration of trend chasers, their predictions are self fulfilling. When their proportion reaches a value close to 55% of the population however the price starts to stagnate, implying a decline in the profitability of this strategy. Next period will then see a lower share of these agents in the market and so on, bursting the bubble.

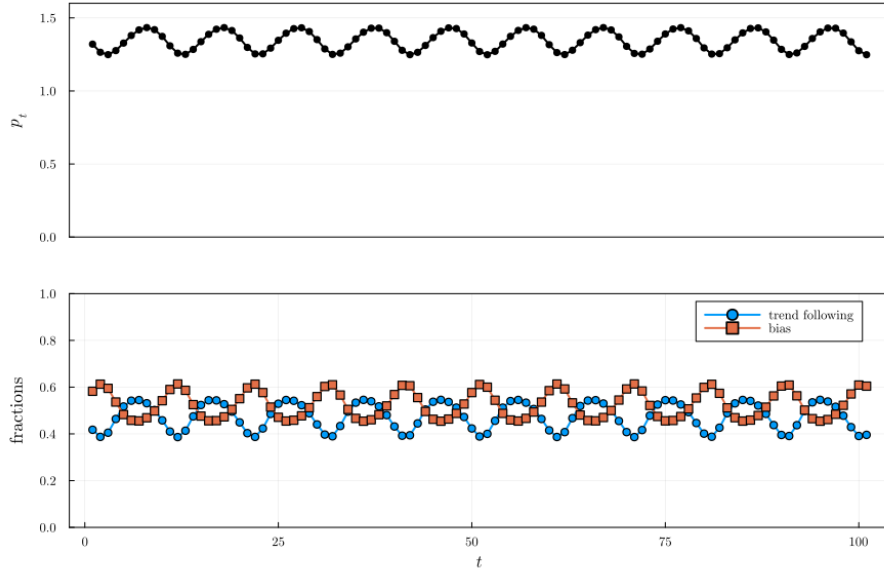


Figure 2: Time series of price deviation (top) and fractions (bottom) for  $\beta = 7.0$

## 2.4 Introducing Speculation

Given the presence of non rational behaviors among investors, classical economic theory would predict that a rational speculator may earn positive returns with its activity, until irrational investors are pushed out of the market, and prices return to rational levels. However, to put it in the words of Keynes: *“Markets can stay irrational longer than you can stay solvent”*. This is especially true in our model in which the fundamental value of the asset is zero which implies that every strictly positive price can be seen as *“irrational”*. We remark again that being rational in an irrational world, is crucially different than being fundamentalist. Moving forward therefore we will compare the two cases: when speculators are fundamentalists and when they take into account the *“irrationality”* of others.

## 2.5 Trend chasers vs pure bias vs fundamentalists

We now study a three type market. The first two strategies are the same as before, the third class of agents are fundamentalists as in (6). The resulting three type model is then given by

$$Rp_t = n_{1,t}gp_{t-1} + n_{2,t}b,$$

with

$$n_{1,t} = \frac{\exp\{\beta\pi_{1,t-1}\}}{\sum_{j=1}^3 \exp\{\beta\pi_{j,t-1}\}}, \quad n_{2,t} = \frac{\exp\{\beta\pi_{2,t-1}\}}{\sum_{j=1}^3 \exp\{\beta\pi_{j,t-1}\}}.$$

As before, we offer a lemma about the existence of steady states of the model.

**Lemma 2 (Steady States of the model with fundamental speculators)** *For  $\beta = 0$ , the model with the fundamentalist speculator has a positive and unique steady state  $p = \frac{b}{3R-g}$ . For  $\beta \rightarrow +\infty$  there are no positive steady states.*

*Proof.* See Appendix B.

We observe that when no switching is present in the model, the resulting steady state is lower than the one in the benchmark two types model. This is consistent with the price reflecting the fundamentalist expectations of the third category of investors. The impact of these agents on global dynamics however is not so straightforward, and we turn again to numerical simulations to analyze it.

## 2.6 Numerical Simulations: $\mathbf{b = 1.0, g = 1.3, R = 1.01}$

Just as before we fix all parameters but the intensity of choice  $\beta$ . In panel (a) of Figure 3 we can observe that the system has a stable steady state for values of the intensity of choice lower than approximately 5.6. After the parameter crosses this value, a bifurcation occurs. Again, in order to characterize this bifurcation and the system dynamics after bifurcation, we use maximum Lyapunov exponents and a plot of the modulus of the system eigenvalues. As we can see in panel (b) of Figure 3 the exponent is negative for low values of  $\beta$  and becomes equal to 0 after the bifurcation. Therefore the system exhibits periodic and quasi periodic orbits, never producing chaos. In panel (c) we plot the modulus of the eigenvalues of the system, that we compute in section (B.4) of the appendix. We can see that just as before for values of  $\beta \approx 5.6$  the two complex eigenvalues cross the unit circle and a Hopf bifurcation occurs. Finally in panel (d) we show the creation of stable orbits after the bifurcation, again allowing us to characterize the bifurcation as super-critical. Two considerations must be made at this point: first, the presence of the fundamentalist type, pushes the overall price closer to the fundamental one. Second, disagreement is added in the system. This causes periodic and quasi periodic orbits to occur for lower values of the intensity of choice, and orbits to have higher amplitude than with respect to the two types model.

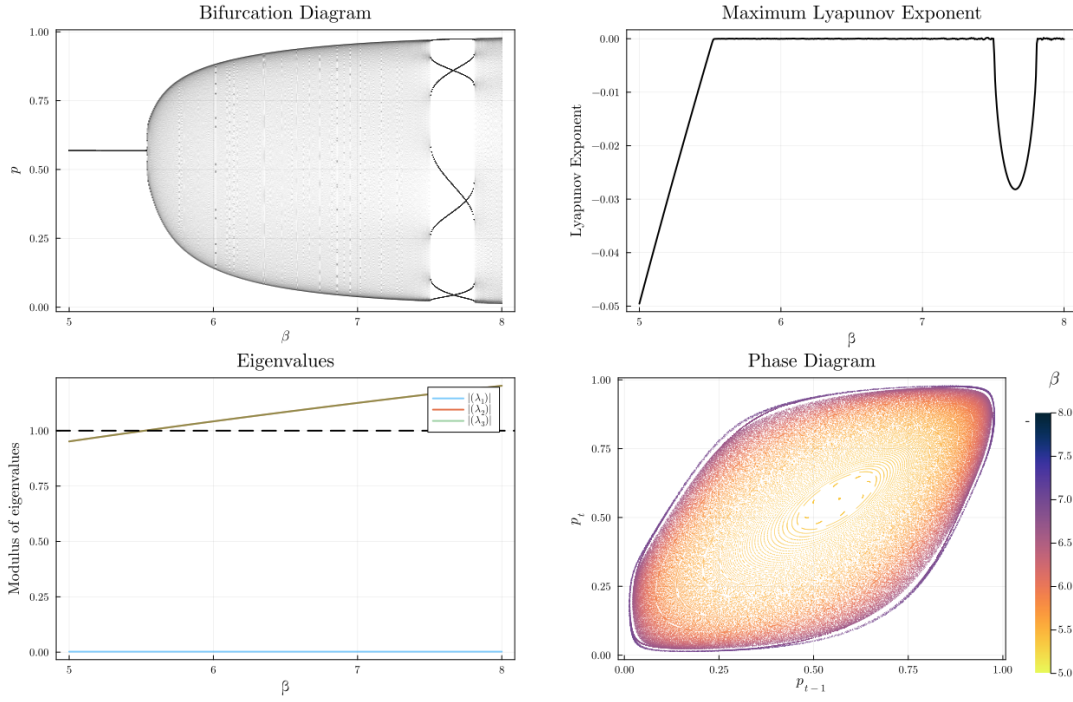


Figure 3: Numerical simulations for the fundamentalist speculation system, other parameters are  $g = 1.3$ ,  $b = 1$ ,  $R = 1.01$ . A Hopf bifurcation occurs for  $\beta \approx 5.6$ , as the two complex eigenvalues have modulus  $|\lambda_2| = |\lambda_3| = 1$ . After the bifurcation periodic and quasi periodic orbits are created.

Figure 4 shows that the dynamic is mainly led by the fundamentalist and the bias categories of investors, while the trend following strategy never being adopted by more than 40% of the model's population. The bubbles now are formed after the price is close the fundamental value. At this point almost all use the fundamentalist strategy. In the next period however the price is going to slowly increase since the few remaining pure bias agents in the market think that the price is extremely low and will demand large quantities. This leads the price to slowly increase and fuel the proportion of trend chasers agents, sustaining the bubble. The burst has similar but reversed story. When the price is high a small fraction of fundamentalist agents think the price is extremely high and sell high quantities of the asset. Pure bias agents are not ready to accommodate this with their demand since the price is already close to what they believe is the proper evaluation of the asset. As a result the bubble collapses and the price starts to go back to the fundamental value.

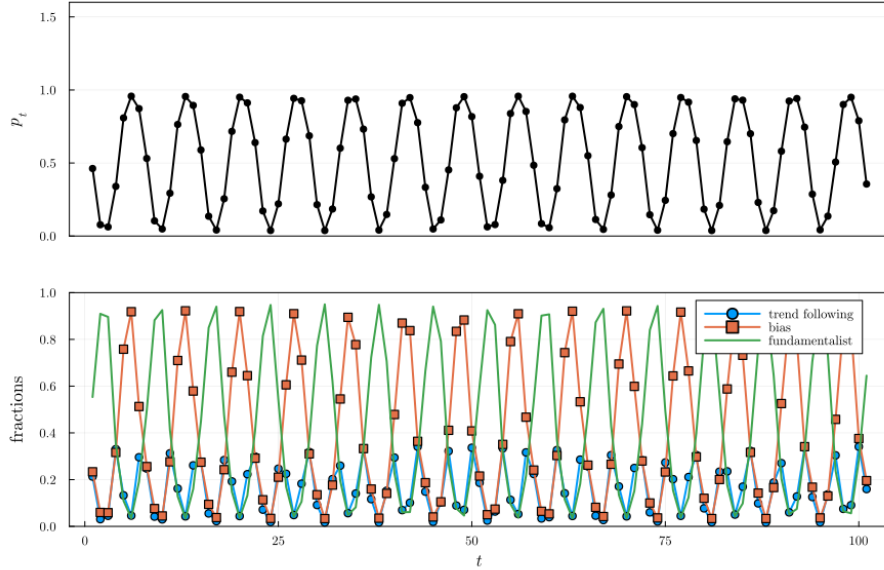


Figure 4: Time series of price deviation (top) and fractions (bottom) for  $\beta = 7.0$

## 2.7 Trend chasers vs pure bias vs rational expectations

We now study a second three types market. The first two strategies are the same but we replace fundamentalists with rational expectations as in equation (7) which gives the following full model (in absence of noise)

$$Rp_t = n_{1,t}gp_{t-1} + n_{2,t}b + n_{3,t}p_{t+1}, \quad (10)$$

with

$$n_{1,t} = \frac{\exp\{\beta\pi_{1,t-1}\}}{\sum_{j=1}^3 \exp\{\beta\pi_{j,t-1}\}}, \quad n_{2,t} = \frac{\exp\{\beta\pi_{2,t-1}\}}{\sum_{j=1}^3 \exp\{\beta\pi_{j,t-1}\}}, \quad n_{3,t} = \frac{\exp\{\beta\pi_{3,t-1}\}}{\sum_{j=1}^3 \exp\{\beta\pi_{j,t-1}\}}.$$

We offer the usual lemma for the existence of steady states for extreme values of the intensity of choice.

**Lemma 3 (Steady States of the model with rational speculators)** *Assume  $\beta = 0$ , then the model with the rational speculator has a positive and unique steady state  $p = \frac{b}{3R-g-1}$ . When  $\beta \rightarrow \infty$ , then the model has no positive steady state.*

*Proof.* See Appendix B.

As before the first observation comes from the case of no switching among strategies. The presence of rational speculators, implies a steady state value slightly lower than in the baseline model. However compared with the three type model with fundamentalist speculator, we observe that the steady state value is much larger. The need for the rational speculator of considering the bias in its forecast, makes so that the model steady state is further away from the fundamental. While in the previous models we were able to provide

numerical simulations effortlessly, this is not possible in this case. The presence of the  $p_{t+1}$  term on the right hand side of equation (10) makes it unfeasible to simulate the model by leveraging established methods from difference equations. To derive rational expectations we then rely on the Extended Path (EP) method proposed by Fair and Taylor (1983)<sup>3</sup>.

### Obtaining Rational Expectations with the Extended Path Method

Before describing the algorithm we find it useful to highlight what we are after and why we need the algorithm in the first place. Start by assuming that expectations formed by the rational agent in the past are indeed rational, that is  $\mathbb{F}_{t-3}(p_{t-1}) = p_{t-1}$ . Then the rational agents needs to choose  $\mathbb{F}_{t-1}(p_{t+1})$  considering the following. After the choice is made, a realization of  $p_t$  is going to be determined by equation (10). Given this and  $\mathbb{F}_t(p_{t+2})$  one can shift (10) forward one period to obtain the realization  $p_{t+1}$ . In order for an agent to have rational expectations we then require  $\mathbb{F}_{t-1}(p_{t+1}) = p_{t+1}$ . Hence when forming expectations at time  $t - 1$  the agents must consider how expectations are going to be formed at time  $t$ . At time  $t$  this is still true, and the agent will have to consider what their expectations are going to be at time  $t + 1$  and so on. Essentially the whole future *path* of expectations is relevant for the choice of expectations today and hence for actual realization of the state variable. We are now ready to describe the algorithm. We are intersted in a path  $\mathcal{P}_t = (p_t, p_{t+1}, \dots, p_{t+T})$ , to obtain it:

- (i) Choose an integer  $k$ , an initial guess of the number of periods beyond the horizon  $T$ , in order to obtain a solution which differs from rational expectations below a tolerance level  $\epsilon$ . Generate an initial expectations vector
$$\mathcal{E}^0 = (p_{t-L}, \dots, p_{t-1}, p_t, p_{t+1}, \dots, p_{t+T}, \dots, p_{t+T+k});$$
- (ii) Use (10) and then shift the resulting vector to obtain
$$\mathcal{E}^1 = (p_{t-L}, \dots, p_{t-1}, p_t, p_{t+1}, \dots, p_{t+T}, \dots, p_{t+T+k});$$
- (iii) Compute the sum of the absolute deviation between  $\mathcal{E}^0$  and  $\mathcal{E}^1$ . If this is less then  $\epsilon$  set  $\mathcal{E}^0 = \mathcal{E}^1$  and return to step (i). Theses iterations are called *Type 1*. Call  $\mathcal{E}_k$  the vector obtained after convergence;
- (iv) Repeat steps (i) to (iii) by replacing  $k$  with  $k + 1$ . Call  $\mathcal{E}_{k+1}$  the vector obtained after convergence. Compute the sum of the absolute deviation between the corresponding elements in  $\mathcal{E}_k$  and  $\mathcal{E}_{k+1}$ . Iterate until it holds that  $|\mathcal{E}_{k+i} - \mathcal{E}_{k+i+1}| < \epsilon$  for some  $i$ . These iterations are called *type 2*;
- (v) The rational *path* vector is given by the corresposding  $T + 1$  elements of the vector  $\mathcal{E}_{k+i}$ .

Now as Fair and Taylor (1983) notice in the original paper “for a general non-linear model there is no guarantee that any of the iterations will converge. If convergence is a problem, it is sometimes helpful to “damp” the successive solution values.” In practice this will be true

---

<sup>3</sup>Boehl and Hommes (2021) recently proposed a new algorithm that achieves higher accuracy compared to the EP in a similar setting. In our specific case we find that the EP obtains a sufficient accuracy and as such using a more sophisticated method is not needed.

in our case when the system enters the unstable region. To deal with this we change the updating mechanism such that the new vector is a convex combination with weights equal to 0.5 of the original vector and of the new one. Finally in order to avoid the algorithm to run forever, we set a maximum of 1000 *type 1* iterations and 100 *type 2* iterations. The parameters of the algorithm that we set are then  $T = 2000$ ,  $\epsilon = e^{-14}$  and  $k = 100$ . In Figure 12 we report the sum of absolute deviations between the rational expectation vector and the realizations of state variables, for increasing values of the intensity of choice  $\beta$  on the x-axis. We can see that although the error is slightly higher in the unstable region, its magnitude is almost always lower than  $8 \times 10^{-15}$ .

## 2.8 Numerical Simulations: $b = 1.0$ , $g = 1.3$ , $R = 1.01$

As with the previous two models we study global dynamics of the system for fixed values of the parameters  $b$ ,  $g$  and  $R$ , and varying the intensity of choice  $\beta$ . In panel (a) of Figure 5 we plot the bifurcation diagram for increasing values of the intensity of choice  $\beta$ . We can observe that the system exhibits a stable steady state for values of the intensity of choice smaller than 6.7. After this value a bifurcation occurs, and the system enters an unstable region. Unfortunately the presence of the rational agents prevents us to analytically compute the eigenvalues of the system, and we can not fully characterize the bifurcation. We can observe however by means of a phase plot in panel (b), that the system exhibits quasi periodic orbits with longer periodicity than with respect to the system with the fundamentalist speculator. In fact the dynamics are similar to those of the two type model.

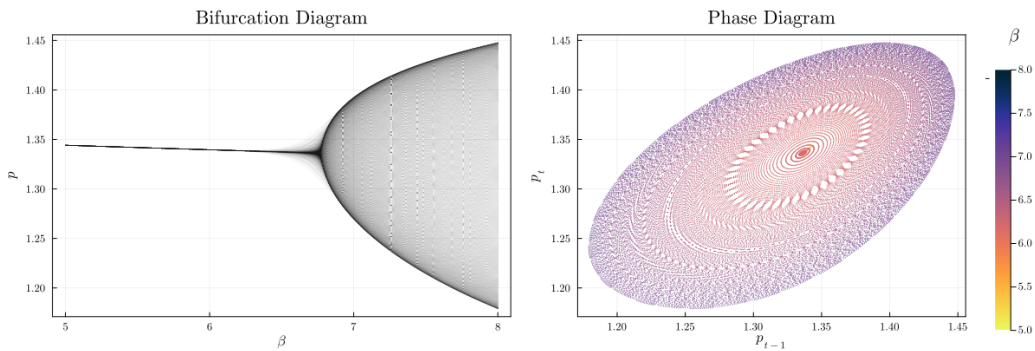


Figure 5: Numerical simulations for the model with rational speculators, other parameters are  $g = 1.3$ ,  $b = 1$ ,  $R = 1.01$ .

The main consideration to make is that unlike the case with the fundamentalist speculators, the system does not approach the fundamental value, even after the bifurcation occurs. To get a better sense of this phenomenon, in Figure 6 we plot the fractions evolution for a value of the intensity of choice  $\beta = 7.0$ .



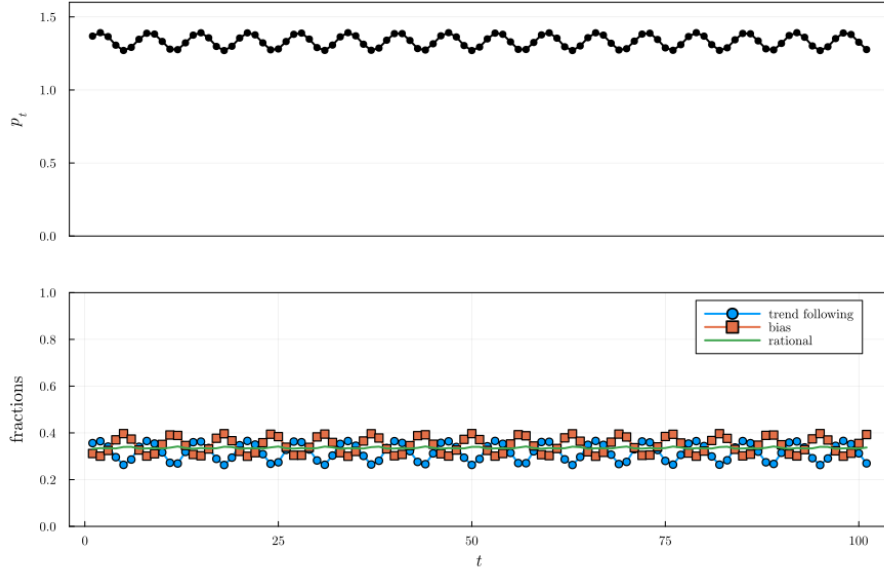


Figure 6: Time series of price deviation (top) and fractions (bottom) for  $\beta = 7.0$

We can see that the fraction of agents using the rational forecast fluctuates significantly less than the other two. Therefore there are two reasons why the resulting price is further away from the fundamental value. The first one is that in order to produce an accurate forecast, rational speculators must take into account the other two agents behavior. This results in a forecast significantly higher than the one a fundamentalist agent would make. The second one is that, as we already remarked, realized profits and forecast accuracy are not perfectly correlated. Speculators using the rational forecast are always present in the system, but they are not able to drive other strategies out of the market. The bubble and bursts motif is similar to the one in the two type models. The bubble is sustained by a growing fractions of trend chasers. Notice however how the fraction of rational agents increases right after the beginning of the bubble and after its collapse. This is the result of this strategy being able to forecast the bursts and booms perfectly. An additional result of this behavior is that the oscillation are dampened as we discuss in the next section.

## 2.9 Speculation Effects

As we can see in Figure 7 the two types of speculation have different effects on the market. When speculators are fundamentalist, they drive prices towards the fundamental benchmark. Their presence though results in increased disagreement, which in turn causes the model to enter the unstable region for lower values of the intensity of choice. Moreover in the unstable region, the resulting volatility is substantially increased. When speculators are rational, we can observe that prices are on average slightly lower than compared with the no speculation case, but still far from the fundamentalist benchmark. An interesting result is that rational speculation decreases volatility in the unstable region with respect to the two type model. This is because speculators can predict the bursting of the bubble and take position before its realization. By doing so they dampen the oscillations in the

market. Rational speculation can have a positive effect on reducing volatility, at the cost of keeping prices further away from the fundamental price that would be achieved in an homogeneous rational world.

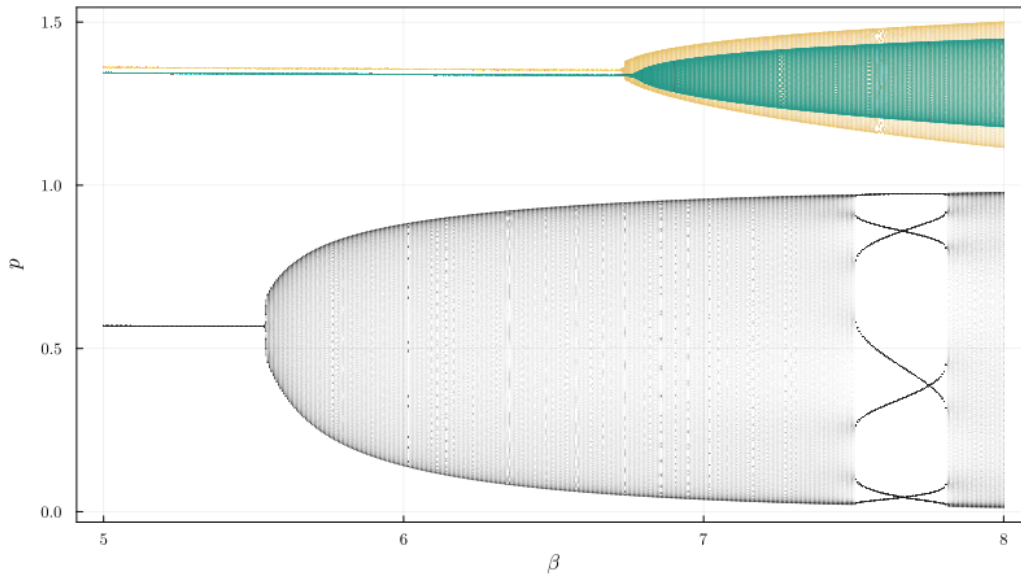


Figure 7: Bifurcation diagrams for all the models

**Note:** The figure shows a bifurcation diagram of the two types model (orange), the model with rational speculators (green) and the one with fundamentalist speculator (black) for increasing values of  $\beta$ . Other parameters are  $g = 1.3$ ,  $b = 1.0$ ,  $R = 1.01$

### 3 Taking the model to the data

In this section, we focus on empirically validating the models previously discussed, utilizing real data from the Bitcoin market.

Our objective is to transition from a static bias to a stochastic measure of bias or sentiment  $w_t$ . To construct a proxy for market sentiment towards Bitcoin, we utilize data from Twitter (currently known as X), assuming that a Tweet conveys part of what a specific investor feel regarding the asset.

We scraped the website for all posts containing the term "Bitcoin" from November 1, 2019, to December 30, 2022. To derive a meaningful sentiment index from this textual data, we used standard preprocessing steps to eliminate stopwords and non-alphabetic characters. We then employed the VADER sentiment analysis library, introduced by [Hutto and Gilbert \(2014\)](#). VADER determines the sentiment of text using a mix of lexical heuristics and a sentiment lexicon, and it can handle idiomatic language and sarcasm. Sentiment scores, ranging from -1 (highly negative) to +1 (highly positive), with 0 indicating neutrality, were computed for each tweet based on the presence of positive, negative, and neutral words. These scores were aggregated daily to form an index labeled Bitcoin Twitter Sentiment Index (BiTSI). Figure 8 shows the evolution of the index and the daily closing price of Bitcoin in US Dollars. To contextualize the index's peaks and troughs, we highlight the

headlines of articles associated with the three highest and lowest BiTSSI values, offering insights into the news events likely driving these sentiment shifts.

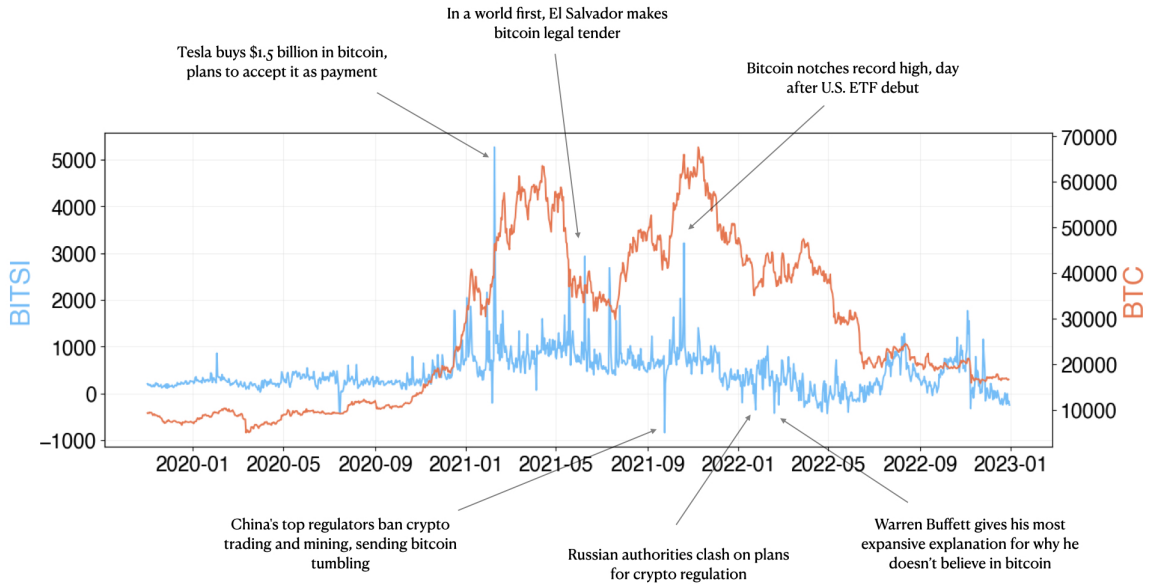


Figure 8: Bitcoin and BiTSSI time series, with relevant events

The index, and the sheer number of tweets per day statistics, are reported in Table 1.

Table 1: Descriptive statistics for the BiTSSI and number of Tweets per day

	<b>BiTSSI</b>	<b>Volume</b>
mean	455.85	8626.90
std	426.51	5160.04
min	-841.15	650
max	5264.47	56179
skew	2.58	1.66
kurtosis	18.58	8.06
obs	1117	1117

As a first analysis we show that our index is not capturing information from other sources highlighted by the literature as having explanatory power on the cryptocurrency return. In a similar fashion to the traditional factor models, [Shen, Urquhart and Wang \(2019\)](#) and [Liu, Tsyvinski and Wu \(2022\)](#) both show that the cross section of cryptocurrencies' excess returns can be substantially explained by three factors: market, size and momentum. In Figure 9 we show correlation among the index and other variables that should proxy at daily level the role of the three factors mentioned above. Excess return is measured as the difference between daily Bitcoin returns and daily risk free rate, represented by the Market Yield on U.S. Treasury Securities at 1-Year Constant Maturity and

available on FRED.<sup>4</sup> We then have two proxies for momentum, given by the first and second difference of daily closing price. Finally 'Volume' represents the daily volume of Bitcoin. All Bitcoin data are gathered from Yahoo Finance. In order to check for the possibility of delayed impact of these factors on the index, we also reported lagged values of all the variables, represented by the '(t-1)' label at the end of the symbol.

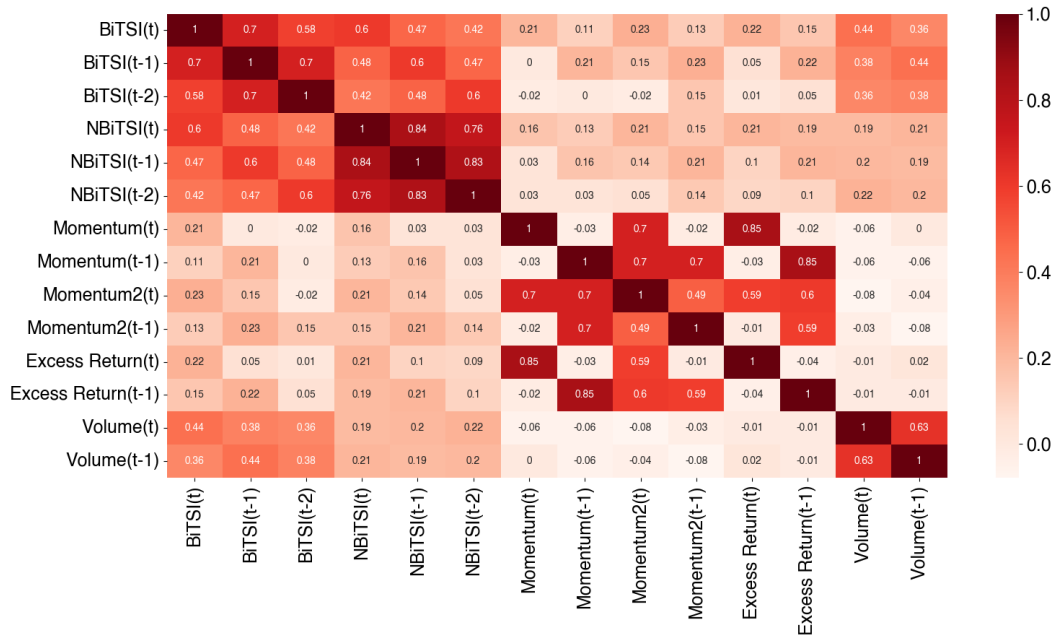


Figure 9: Correlation of the BiTSI and other variables

The correlation between the index and all the other variables is mostly positive and relatively small, except the one with Volume. The result is however explained by the correlation, already documented in the literature, between Bitcoin volume and Tweet volume. This is why we also include the Normalised BiTSI, where the normalization factor is the volume of Tweets per day. After removing the magnitude effect, the index appears to be only mildly correlated to the variables.

## 4 Estimating Non-linear Rational Expectation models with a Neural Network

We turn now to the estimation of the three models introduced above. While the first two are straightforward to estimate via Non Linear Least Squares (NLS), the model with rational speculators requires obtaining rational expectations first. In their paper [Fair and Taylor \(1983\)](#) propose a maximum likelihood estimation which is built on the EP algorithm. The idea is to first solve the model for rational expectations given a choice of the parameters. After obtaining the rational expectations vector one can compute the log-likelihood associ-

<sup>4</sup>The yearly rate is then transformed in the corresponding daily one by  $r_{daily} = r_{yearly}/365$ . The choice is motivated by the yearly capitalization of the instrument.

ated with the parameters. In order to obtain the optimal estimates one has therefore to apply the EP algorithm for every possible combinations of parameters in a specific grid. This can be computationally expensive as in our case we are interested in the three behavioral parameters,  $g$ ,  $b$  and  $\beta$  and would require a high grid density given the highly non-linear structure of the problem. To summarize their procedure suffers from the *curse of dimensionality* as every extra parameters to be estimated exponentially increases the computational time. To deal with this we propose a procedure which consists of two ingredients. The first is to ensure that we can express the state variable as a function of past states only. A general formulation for our specific problem is of the form

$$p_t = \mathcal{F}(\{p_{t-l}\}_{l=0}^L, \{\mathbb{E}_t(p_{t+k})\}_{k=1}^K, \{w_{t-l}\}_{l=0}^L; \alpha) + \varepsilon_t$$

and we want to estimate the parameter vector  $\alpha$ . First we follow [Fair and Taylor \(1983\)](#) in setting all future disturbances  $\varepsilon_t$  equal to their conditional mean in a deterministic model. This is needed since in a non-linear rational model, conditional expectations will involve higher order moments. As there is no ex ante way of assessing the goodness of this approximation for a general non linear model, we can only assess that in practice this is sufficient for our case. Therefore we focus on

$$p_t = \mathcal{F}(\{p_{t-l}\}_{l=0}^L, \{p_{t+k}\}_{k=1}^K, \{w_{t-l}\}_{l=0}^L; \alpha) + \varepsilon_t$$

Defining by  $\mathcal{F}^{(n)}$  the function obtained from  $\mathcal{F}$  by iterating all future expectations of the state variables  $n-1$  times. We can easily see that if

$$\lim_{n \rightarrow +\infty} \frac{\partial \mathcal{F}^{(n)}}{\partial p_{t+k}} \rightarrow 0, \text{ for all } k > 0,$$

and there exist a finite  $M$  such that

$$p_{t+k} \in [-M, M], \text{ for all } k > 0,$$

then there exist a generic function  $\mathcal{H}$  of past states only, a  $N$  and an  $\epsilon > 0$  such that for all  $n > N$

$$\left| \mathcal{F}^{(n)}(\{p_{t-l}\}_{l=0}^L, \{p_{t+k}\}_{k=0}^K, \{w_{t-l}\}_{l=0}^L; \alpha) - \mathcal{H}(\{p_{t-l}\}_{l=0}^L, \{w_{t-l}\}_{l=0}^L; \alpha) \right| < \epsilon$$

This ensures that iterating the function with respect to future variables, we eventually reach a point after which the impact of the future on today is negligible. Unfortunately showing that a general function  $\mathcal{F}$  satisfies the assumption is not trivial in non linear cases.<sup>5</sup> We can only assess that in practice this condition is likely to be met for realistic values of the parameters.

The second ingredient is that of obtaining an approximation to the unknown function

---

<sup>5</sup>For a detailed discussion we can refer to [Boehl and Hommes \(2021\)](#)

$\mathcal{H}$  via a Neural Network (NN), that is reparametrizing

$$\mathcal{H}(\{p_{t-l}\}_{l=0}^L, \{w_{t-l}\}_{l=0}^L; \alpha) \approx \hat{\mathcal{H}}(\{p_{t-l}\}_{l=0}^L, \{w_{t-l}\}_{l=0}^L; \theta),$$

where now  $\theta$  are the parameters of the NN. We deem this appropriate as it was shown in [Hornik, Stinchcombe and White \(1989\)](#) that multilayer feedforward networks are universal approximators.

We now specialize to the case at our hand. Start from

$$p_t = \mathcal{F}(p_{t-1}, p_{t-2}, p_{t-3}, p_{t+1}, w_{t-1}, w_{t-3}; \alpha).$$

we get

$$p_{t+1} = \mathcal{H}(p_{t-1}, p_{t-2}, p_{t-3}, w_{t-1}, w_{t-2}, w_{t-3}; \alpha),$$

and approximate it via a NN

$$p_{t+1} = \hat{\mathcal{H}}(p_{t-1}, p_{t-2}, p_{t-3}, w_{t-1}, w_{t-2}, w_{t-3}; \theta),$$

with architecture described in [Appendix E](#). After obtaining a vector of rational expectations  $\{\mathbb{E}_{t-l}(p_{t+1-l})\}_{l=1}^L$  we can proceed with estimation. To show that our method is indeed able to obtain a satisfactory approximation of rational expectations we use the following exercise. We generate synthetic data for the model with trend chasers vs pure bias vs rational speculators, for two values of the intensity of choice  $\beta \in \{3.0, 7.0\}$  corresponding to the stable and unstable region and keeping all other parameters fixed at their level of  $g = 1.3$ ,  $b = 1.0$ ,  $R = 1.01$ . For each of these two regions, we generate a model with a Noise to Signal ratio of 0 (corresponding to the deterministic case), 0.01 and 0.1. We then train the NN on the synthetic data and show the Mean Squared Error (MSE) between the NN estimates and the true rational expectations vector. Then, using the NN estimates, we estimate the three parameters  $g$ ,  $b$  and  $\beta$  with NLS and report the point estimate and the associated standard errors in parentheses. Results are shown in [Table 2](#).

Table 2: Estimation on syntethic data

	Stable region, $\beta = 3$			Unstable region, $\beta = 7$		
N/S	0	0.01	0.1	0	0.01	0.1
MSE	0.0000	0.0009	0.0009	0.0037	0.0050	0.0235
$g$	1.17 (0.00)	1.26 (0.03)	1.26 (0.03)	1.29 (0.00)	1.25 (0.02)	1.10 (0.01)
$b$	1.17 (0.00)	1.07 (0.04)	1.07 (0.04)	1.01 (0.00)	1.05 (0.02)	1.11 (0.02)
$\beta$	0.88 (0.00)	3.10 (0.89)	3.07 (0.88)	7.40 (0.05)	6.79 (1.02)	8.85 (1.28)

We can see that the NN is able to approximate the rational expectations vector with a low Mean Squared Error. Clearly the approximation deteriorating when the Noise to Signal ratio increasing. This however does not seem to impair the estimation. Estimates for the  $g$  and  $b$  parameter are close to their true value, with the noticeable exception of



the first column. When the dynamics are stable and there is no noise, there is simply no variance to estimate correctly the parameter values. The estimation of the intensity of choice parameter is the one associated with the higher standard errors. This is in line with findings in the literature [Boswijk, Hommes and Manzan \(2007\)](#), [ter Ellen, Hommes and Zwinkels \(2021\)](#) documenting that the pinning down of the parameter is hard to achieve. The reason is that large changes in this parameter have only mild effects on the overall fractions, given the smoothness of the multinomial logit function. In any case we find that the point estimate is always in the confidence interval, except when no noise is present.

## 5 Estimation

We now turn to the estimation of real data. We accommodate some changes to allow the incorporation of financial data into the theoretical model. First, we incorporate a time varying risk-free rate, as proxied by the Market Yield on U.S. Treasury Securities at 1-Year Constant Maturity discussed above so that instead of having a fixed  $R$  we have a time varying  $R_t$ . Second we deal with the non-stationarity of the data. We follow [ter Ellen, Hommes and Zwinkels \(2021\)](#) in rewriting the model in deviation from a moving average

$$\text{MA}_t = \frac{\sum_{i=W}^1 p_{t-i}}{W}$$

where  $W$  is the window size, so that our state variable is  $x_t = p_t - \text{MA}_t$ . In the baseline we fix it to 40 days. We discuss the sensitivity of the estimation to this choice in Appendix G. Third, we need to deal with numerical overflows in the estimation caused by taking exponents of large profits when computing the fractions. We do this by assuming that the subjective variance of the variable our agents needs to forecast is homogeneously equal to the square of the last available moving average  $(\text{MA}_{t-3})^2$ . Lastly we deal with heteroskedasticity of residuals by rewriting the model in percentage deviation from the moving average fundamental, by simply dividing both sides of the pricing equation by the fundamental value itself.

The model we take to the data is then the following

$$R_t \frac{x_t}{\text{MA}_t} = n_{1,t} g \frac{x_{t-1}}{\text{MA}_t} + n_{2,t} b \frac{w_{t-1}}{\text{MA}_t} + n_{3,t} \frac{\mathbb{F}_{3,t}(x_{t+1})}{\text{MA}_t},$$

where  $n_{3,t}$  will be 0 in the two types model, and  $\mathbb{F}_{3,t}(x_{t+1})$  will be 0 in the fundamental case and the output of the Neural Network model in the rational one.

Fractions are given as the usual multinomial logit, where now the fitness measure is given by

$$\pi_{1,t} = \frac{1}{\text{MA}_{t-3}^2} (x_t - R_{t-2}x_{t-1}) (gx_{t-3} - R_{t-2}x_{t-1}),$$

$$\pi_{2,t} = \frac{1}{\text{MA}_{t-3}^2} (x_t - R_{t-2}x_{t-1}) (bw_{t-3} - R_{t-2}x_{t-1}),$$

$$\pi_{3,t} = \frac{1}{\text{MA}_{t-3}^2} (x_t - R_{t-2}x_{t-1}) (\mathbb{F}_{3,t-2}(x_{t-1}) - R_{t-2}x_{t-1}),$$

which are the usual profits divided by the square of the moving average fundamental. We use this non centered second moment as a time varying proxy of the volatility of the asset.

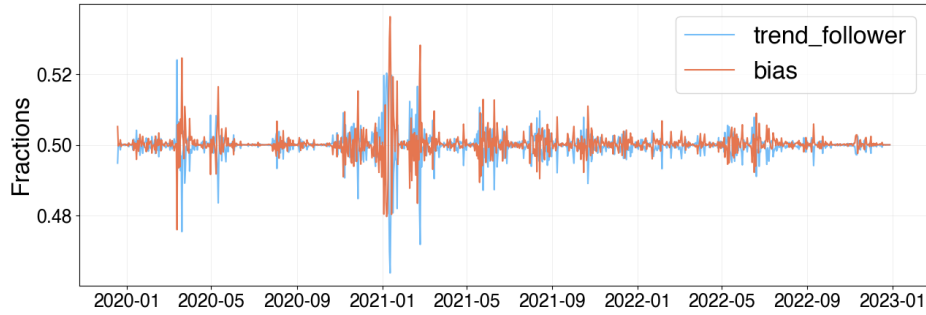
We then plot and test the variables for stationarity in Appendix F.

We finally estimate the parameters  $g$ ,  $b$  and  $\beta$  for the three model presented by NLS. Results are reported in Table 3.

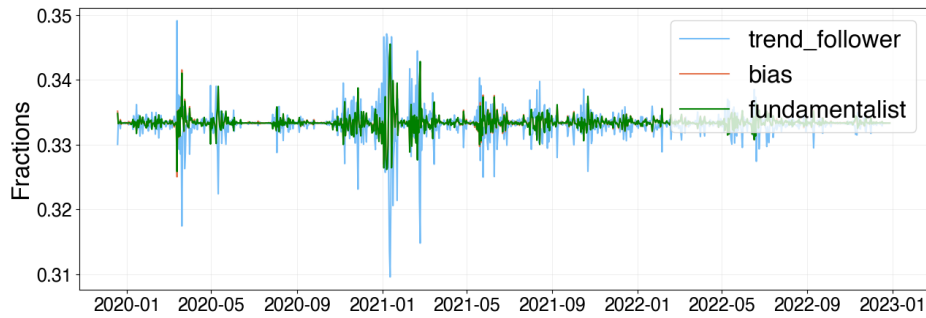
Table 3: Estimation results

	Trend chasers vs pure bias	Tc vs B vs Fundamentalist	Tc vs B vs Rational Expectations
$g$	1.91 (121.66)	2.86 (121.51)	1.92 (84.14)
$b$	0.58 (6.5)	0.87 (6.5)	0.83 (6.41)
$\beta$	1.03 (2.12)	0.51 (2.14)	1.45 (2.05)
Adj $r^2$	0.94	0.94	0.94
F-stat	4.61 (0.03)	4.74 (0.03)	4.34 (0.04)
het	0.17	0.17	0.11

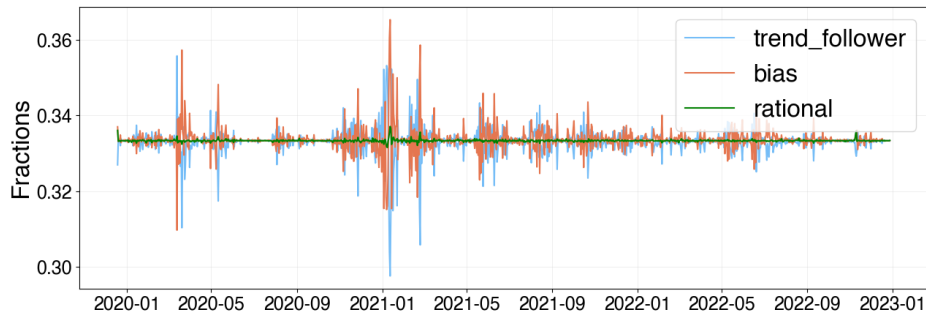
We report the point estimate of the parameters and the associated t-statistic in parentheses. We also report the adjusted R-squared value, and the value and associated p-value of the F-test for the significance of the non-linear model with respect to a linear one. This can be seen as nested in the non-linear model and corresponding to a value of the intensity of choice  $\beta$  equal to 0. Lastly we report the p-value associated with the Engle’s Test for Autoregressive Conditional Heteroscedasticity on the estimation residuals. The null hypothesis in the test is that of homoskedasticity and we can not reject it in all specifications given the p-values. Nonetheless we run the estimation again by obtaining confidence interval for the parameters by an heteroskedasticity robust bootstrap procedure in Appendix H. The first type of investors are strong trend chasers, expecting deviations from fundamentals to continue with increased magnitude in the subsequent periods. This is in line with psychological aspects, like “fear of missing out” (FOMO) which is extremely relevant in the cryptocurrency market and documented for example by [Baur and Dimpfl \(2018\)](#). Their extrapolation becomes highest in the model with fundamentalist agent. This can be explained by the presence of a type of investor in the model that always forecasts the fundamental price, therefore absorbing part of what before we might have classified as mild trend chasers. The second category of investors can be classified as weakly sentiment followers, as they constantly expect a small deviation from the fundamental moving average which is positively proportional to the sentiment index. The F-test confirms in every case evidence of non-linearities, at least at the 5% level. The small but significance estimate for  $\beta$  implies long periods of coexistence of different strategies in the market. However as we can see from Figure 10 there are periods of substantial switching. We conjecture that the result is due to the proximity of the intensity of choice to the bifurcation. Large enough shocks can temporarily affect the stability of the steady state and drive the model in the unstable region, with a resulting volatility amplification that can last for several days.



(a) Trend chasers vs pure bias



(b) Trend chasers vs pure bias vs fundamentalists



(c) Trend chasers vs pure bias vs rational expectations

Figure 10: Fractions evolution for estimated parameters

## 6 Conclusion and Discussion

In this paper we have proposed a heterogeneous agent asset pricing model with different categories of investors endogenously evolving over time. The presence of boundedly rational investors in the market, with trend following and bias forecasting rules, raises the question about speculation opportunities. We have introduced two different types of speculation. The first one is associated with fundamentalist traders, that know the true underlying process of the asset and behave accordingly. We remarked however that to have rational expectations in our model one has to take into account the (possibly incorrect) strategies of other investors. We show that when speculators are of the second type, the

resulting price is further away from the fundamental price but volatility is reduced compared to the fundamentalist speculation benchmark. Hence rational speculators have a stabilising effect on the market. The second part of the paper is devoted to provide empirical support to our model. We opted to use data from the Bitcoin market and constructed the BiTSI index, that we used as a proxy of a time evolving bias. The BiTSI index is shown to capture an aspect of the market which is uncorrelated with the main factors highlighted by the literature in explaining Bitcoin returns. To estimate the non-linear dynamic rational expectation model we proposed a methodology using a Neural Network which overcomes the curse of dimensionality. We showed that this method provides a satisfactory approximation of rational expectations on synthetic data. After estimating the models by Non Linear Least Squares we found evidence of the coexistence of multiple strategies in the market and of mild switching.

## References

- Aalborg, Halvor Aarhus, Peter Molnár, and Jon Erik de Vries.** 2019. "What can explain the price, volatility and trading volume of Bitcoin?" *Finance Research Letters*, 29.
- Adam, Klaus, and Stefan Nagel.** 2023. "Chapter 16 - Expectations data in asset pricing."
- Armstrong, John, Richard Black, Douglas Laxton, and David Rose.** 1998. "A robust method for simulating forward-looking models." *Journal of Economic Dynamics and Control*, 22.
- Baig, Ahmed, Benjamin M. Blau, and Nasim Sabah.** 2019. "Price clustering and sentiment in bitcoin." *Finance Research Letters*, 29.
- Baur, Dirk G., and Kristoffer J. Glover.** 2014. "Heterogeneous expectations in the gold market: Specification and estimation." *Journal of Economic Dynamics and Control*, 40.
- Baur, Dirk G., and Thomas Dimpfl.** 2018. "Asymmetric volatility in cryptocurrencies." *Economics Letters*, 173.
- Benettin, Giancarlo, Luigi Galgani, Antonio Giorgilli, and Jean-Marie Strelcyn.** 1980. "Lyapunov Characteristic Exponents for smooth dynamical systems and for Hamiltonian systems; a method for computing all of them. Part 1: Theory." *Meccanica*, 15(1): 9–20.
- Boehl, Gregor, and Cars Hommes.** 2021. "Rational vs. Irrational Beliefs in a Complex World." *Discussion Paper No. 287 Project C 01*, Discussion Paper Series – CRC TR 224.
- Bolt, Wilko, Maria Demertzis, Cees Diks, Cars Hommes, and Marco van der Leij.** 2019. "Identifying booms and busts in house prices under heterogeneous expectations." *Journal of Economic Dynamics and Control*, 103.

- Boswijk, H. Peter, Cars H. Hommes, and Sebastiano Manzan.** 2007. "Behavioral heterogeneity in stock prices." *Journal of Economic Dynamics and Control*, 31.
- Bourghelle, David, Fredj Jawadi, and Philippe Rozin.** 2022. "Do collective emotions drive bitcoin volatility? A triple regime-switching vector approach." *Journal of Economic Behavior & Organization*, 196.
- Brock, William A., and Cars H. Hommes.** 1997. "A Rational Route to Randomness." *Econometrica*, 65.
- Brock, William A., and Cars H. Hommes.** 1998. "Heterogeneous beliefs and routes to chaos in a simple asset pricing model." *Journal of Economic Dynamics and Control*, 22.
- Brock, William A., Cars H. Hommes, and Florian O.O. Wagener.** 2005. "Evolutionary dynamics in markets with many trader types." *Journal of Mathematical Economics*, 41.
- Cheah, Eng Tuck, and John Fry.** 2015. "Speculative bubbles in Bitcoin markets? An empirical investigation into the fundamental value of Bitcoin." *Economics Letters*, 130.
- Chen, Cathy Yi Hsuan, and Christian M. Hafner.** 2019. "Sentiment-Induced Bubbles in the Cryptocurrency Market." *Journal of Risk and Financial Management*, 12.
- Chiarella, Carl, Saskia ter Ellen, Xue Zhong He, and Eliza Wu.** 2014. "Fear or fundamentals? Heterogeneous beliefs in the European sovereign CDS market." *Journal of Empirical Finance*, 32.
- Chiarella, Carl, Xue Zhong He, and Remco C.J. Zwinkels.** 2014. "Heterogeneous expectations in asset pricing: Empirical evidence from the S&P500." *Journal of Economic Behavior and Organization*, 105.
- Cornea-Madeira, Adriana, Cars Hommes, and Domenico Massaro.** 2019. "Behavioral Heterogeneity in U.S. Inflation Dynamics." *Journal of Business and Economic Statistics*, 37.
- De Long, J. Bradford, Andrei Shleifer, Lawrence H. Summers, and Robert J. Waldmann.** 1990. "Noise Trader Risk in Financial Markets." *Journal of Political Economy*, 98.
- Fair, Ray C., and John B. Taylor.** 1983. "Solution and Maximum Likelihood Estimation of Dynamic Nonlinear Rational Expectations Models." *Econometrica*, 51.
- Fisher, P. G., S. Holly, and A. J. Hughes Hallett.** 1986. "Efficient solution techniques for dynamic non-linear rational expectations models." *Journal of Economic Dynamics and Control*, 10.
- Franke, Reiner, and Frank Westerhoff.** 2012. "Structural stochastic volatility in asset pricing dynamics: Estimation and model contest." *Journal of Economic Dynamics and Control*, 36.

- Frijns, Bart, Thorsten Lehnert, and Remco C.J. Zwinkels.** 2010. "Behavioral heterogeneity in the option market." *Journal of Economic Dynamics and Control*, 34.
- Goncalves, Silvia, and Lutz Kilian.** 2004. "Bootstrapping autoregressions with conditional heteroskedasticity of unknown form." *Journal of Econometrics*, 123.
- Goodfellow, Ian, Yoshua Bengio, and Aaron Courville.** 2016. *Deep Learning*. MIT Press.
- Gurdgiev, Constantin, and Daniel O'Loughlin.** 2020. "Herding and anchoring in cryptocurrency markets: Investor reaction to fear and uncertainty." *Journal of Behavioral and Experimental Finance*, 25.
- Guégan, Dominique, and Thomas Renault.** 2021. "Does investor sentiment on social media provide robust information for Bitcoin returns predictability?" *Finance Research Letters*, 38.
- Harris, M., and A. Raviv.** 1993. "Differences of opinion make a horse race." *Review of Financial Studies*, 6.
- He, Xue Zhong, and Kai Li.** 2012. "Heterogeneous beliefs and adaptive behaviour in a continuous-time asset price model." *Journal of Economic Dynamics and Control*, 36.
- Hommes, Cars.** 2021. "Behavioral and experimental macroeconomics and policy analysis: A complex systems approach." *Journal of Economic Literature*, 59.
- Hommes, Cars, Hai Huang, and Duo Wang.** 2005. "A robust rational route to randomness in a simple asset pricing model." *Journal of Economic Dynamics and Control*, 29.
- Hommes, Cars, Joep Sonnemans, Jan Tuinstra, and Henk Van De Velden.** 2005. "Coordination of expectations in asset pricing experiments." *Review of Financial Studies*, 18.
- Hong, Harrison, and Jeremy C. Stein.** 2003. "Differences of Opinion, Short-Sales Constraints, and Market Crashes." *Review of Financial Studies*, 16.
- Hornik, Kurt, Maxwell Stinchcombe, and Halbert White.** 1989. "Multilayer feedforward networks are universal approximators." *Neural Networks*, 2.
- Hutto, Clayton J., and Eric Gilbert.** 2014. "VADER: A Parsimonious Rule-based Model for Sentiment Analysis of Social Media Text." *International Conference on Web and Social Media*.
- Jegadeesh, Narasimhan, and Sheridan Titman.** 1993. "Returns to Buying Winners and Selling Losers: Implications for Stock Market Efficiency." *Journal of Finance*, 48.
- J.Parra-Moyano, D.Partida, M. Gessl, and S.Mazumdar.** 2024. "Analyzing swings in Bitcoin returns: a comparative study of the LPPL and sentiment-informed random forest models." *Digital Finance*, 6.



- Liu, Yukun, Aleh Tsyvinski, and Xi Wu.** 2022. "Common Risk Factors in Cryptocurrency." *The Journal of Finance*, 77.
- Liu, Yukun, and Aleh Tsyvinski.** 2020. "Risks and returns of cryptocurrency." *Review of Financial Studies*, 34.
- Lof, Matthijs.** 2015. "Rational speculators, contrarians, and excess volatility." *Management Science*, 61.
- Makarov, Igor, and Antoinette Schoar.** 2020. "Trading and arbitrage in cryptocurrency markets." *Journal of Financial Economics*, 135.
- Manski, C., and D. McFadden.** 1981. *Alternative Estimators and Sample Designs for Discrete Choice Analysis*. The MIT Press.
- Muth, John F.** 1961. "Rational Expectations and the Theory of Price Movements." *Econometrica*, 29.
- Schmitt, Noemi.** 2021. "Heterogeneous expectations and asset price dynamics." *Macroeconomic Dynamics*, 25.
- Shalen, Catherine T.** 1993. "Volume, Volatility, and the Dispersion of Beliefs." *Review of Financial Studies*, 6.
- Shen, Dehua, Andrew Urquhart, and Pengfei Wang.** 2019. "A three-factor pricing model for cryptocurrencies." *Finance Research Letters*, 34.
- ter Ellen, Saskia, Cars H. Hommes, and Remco C.J. Zwinkels.** 2021. "Comparing behavioural heterogeneity across asset classes." *Journal of Economic Behavior and Organization*, 185.
- Urquhart, Andrew.** 2016. "The inefficiency of Bitcoin." *Economics Letters*, 148.
- Urquhart, Andrew.** 2018. "What causes the attention of Bitcoin." *Economics Letters*, 166.

## A Micro-foundation of the Brock and Hommes (1998) Model

Consider an overlapping generation model. The economy is populated by  $N$  agents living two periods. When young agents receive  $w_0$  units of consumption good. When old they consume all of their wealth, with a utility function given by

$$U(c_{t+1}) = -e^{-ac_{t+1}},$$

where  $a > 0$  is the coefficient of absolute risk aversion. Agents can choose between two types of securities to transfer wealth from the first period to the second. They can use a riskless asset, which pays fixed interest  $R > 1$  for each unit of saved good or alternatively they can use a risky asset. Agents pay price  $p_t$  to purchase the asset at time  $t$ , and when old they obtain the payoff  $y_{t+1} = p_{t+1} + d_{t+1}$ . This is given by the price at which they can sell the asset  $p_{t+1}$  plus a dividend claim  $d_{t+1}$  which is assumed to be constant plus normal white noise. In our specific setting we will assume it constantly equal to 0 so that going forward  $y_{t+1} = p_{t+1}$ . Agents need to choose their demand of the risky asset, defined by  $z_t^d$ , in order to maximize their utility, subject to the following budget constraint

$$c_{t+1} = R(w_0 - p_t z_t^d) + z_t^d p_{t+1}.$$

All agents assume that  $c_{t+1}$  is normally distributed, then their utility maximization problem, is equivalent to

$$\max_{\{z_t^d\}} \left( -\exp \left\{ -a \mathbb{E}_t(c_{t+1}) + \frac{a^2}{2} \mathbb{V}_t(c_{t+1}) \right\} \right). \quad (11)$$

Exploiting the budget constraint we have that

$$\mathbb{E}_t(c_{t+1}) = R(w_0 - p_t z_t^d) + z_t^d \mathbb{E}_t(p_{t+1}),$$

and

$$\mathbb{V}_t(c_{t+1}) = (z_t^d)^2 \mathbb{V}_t(p_{t+1}).$$

Then the optimal choice of the risky asset must satisfy the first order condition of equation (11).

$$z_t^d = \frac{\mathbb{E}_t(p_{t+1}) - R p_t}{a \mathbb{V}_t(p_{t+1})}.$$

To get a solution for the price  $p_t$  we impose the equilibrium condition that demand must equal supply  $z_t^s$ . Finally we assume net supply of the risky asset is 0 to get

$$\frac{\mathbb{E}_t(p_{t+1}) - R p_t}{a \mathbb{V}_t(p_{t+1})} = 0. \quad (12)$$

From equation (12) we can notice that if agents had homogenous beliefs, therefore sharing the same expected value and variance of the asset, the pricing equation would be

$$Rp_t = \mathbb{E}_t(p_{t+1}). \quad (13)$$

Equation (13) has two class of solutions, usually referred to as fundamentalist and rational bubble solution. The fundamental price is  $p_t \equiv \bar{p} = 0$  in each time step, where  $r = R - 1$  is the net free-rate. Whereas the rational bubble price is  $\tilde{p}_t = \zeta_t R^{-t}$  where  $\zeta_t$  is any martingale process. Now consider J different types of agents, with different expectation formation processes regarding the future price of the risky asset. The equilibrium pricing equation (12) becomes

$$\sum_{j=1}^J \left( n_{j,t} \cdot \frac{\mathbb{F}_{j,t}(p_{t+1}) - Rp_t}{a \mathbb{V}_{j,t}(p_{t+1})} \right) = 0,$$

where  $\mathbb{F}_{j,t}(p_{t+1})$  and  $\mathbb{V}_{j,t}(p_{t+1})$  indicate the subjective expectation and variance of agent j and  $n_{j,t}$  represents the fraction of agents using strategy j. Finally we make the assumption of constant beliefs on variance:  $\mathbb{V}_{j,t}(p_{t+1}) = \sigma_p^2, \forall j$ .<sup>6</sup> With this assumption the equilibrium price is given by

$$Rp_t = \sum_{j=1}^J n_{j,t} \cdot \mathbb{F}_{j,t}(p_{t+1}).$$

Fractions are updated every period according to a fitness measure that is public knowledge and is given by profits or returns in excess of the risk-free rate are given by

$$\pi_{j,t} = (p_t - Rp_{t-1}) z_{t-1}^d,$$

finally assuming that  $a\sigma_p^2 = 1$  we get the expression in equation (2).

## B Proofs

### B.1 Proof of Lemma 1 (See page 7)

Steady states of the system must solve

$$Rp = n_1 gp + (1 - n_1)b,$$

where

$$n_1 = \frac{1}{1 + \exp\{\beta(p - Rp)(b - gp)\}},$$

and satisfy the constraint on the parameters  $b > 0, g > 0, R > 1$ . When  $\beta = 0$  then  $n_1 = \frac{1}{2}$  for all p which implies that  $p = \frac{b}{2R-g}$ . The stability of the system can be determined by

---

<sup>6</sup>Although we shall overlook this second-order effect, it should be noted that heterogeneity in conditional expectations does, in fact, cause heterogeneity in conditional variance. Again we refer to [Brock and Hommes \(1998\)](#) for a more thorough discussion.

studying the first order difference equation

$$p_t = \frac{g}{2R}p_{t+1} + \frac{b}{2R},$$

and imposing

$$\left| \frac{dp_t}{p_{t-1}} \right| = \left| \frac{g}{2R} \right| < 1.$$

Since we are working under the assumption that  $g > 0$  and  $R > 1$  the steady state is then locally stable for  $g < 2R$ .

When  $\beta = +\infty$  the price function is piecewise defined as

$$p_t = \begin{cases} \frac{g}{R}p_{t-1} & \text{for } \Delta\pi_{t-1} < 0 \\ \frac{g}{2R}p_{t-1} + \frac{b}{2R} & \text{for } \Delta\pi_{t-1} = 0 \\ \frac{b}{R} & \text{for } \Delta\pi_{t-1} > 0 \end{cases}$$

where  $\Delta\pi_{t-1} = (p_{t-1} - Rp_{t-2})(b - gp_{t-3})$ , is the difference in realized profits between the bias traders and the trend following traders. To obtain the steady states and their stability we can then proceed by cases

(i)  $\Delta\pi_{t-1} < 0$ . Then a steady state  $p$  must satisfy the following pair of equations

$$\begin{cases} p = \frac{g}{R}p \\ (p - Rp)(b - gp) < 0 \end{cases}$$

which has solution if and only if  $g = R$  with  $p < \frac{b}{R}$ . The steady state stability is determined by

$$\left| \frac{dp_t}{p_{t-1}} \right| = \left| \frac{g}{R} \right| = 1,$$

therefore the steady state is locally unstable.

(ii)  $\Delta\pi_{t-1} = 0$ . Then a steady state  $p$  must satisfy the following pair of equations

$$\begin{cases} p = \frac{g}{2R}p + \frac{b}{2R} \\ (p - Rp)(b - gp) = 0 \end{cases}$$

Since  $b > 0$ , a solution in this case exists if and only if  $g = R$  which then leads to  $p = b/R = b/g$ . The stability of this solution is given by

$$\left| \frac{dp_t}{p_{t-1}} \right| = \left| \frac{g}{2R} \right| = \left| \frac{1}{2} \right| < 1,$$

which implies that the steady state is locally stable.

(iii)  $\Delta\pi_{t-1} > 0$ . Then a steady state  $p$  must satisfy the following pair of equations

$$\begin{cases} p = \frac{b}{R} \\ (p - Rp)(b - gp) > 0 \end{cases}$$

The solution  $p = \frac{b}{R}$  can be sustained only if  $g > R$  since  $b > 0$ . The stability of the steady state is regulated by

$$\left| \frac{dp_t}{p_{t-1}} \right| = 0,$$

implying a locally stable steady state.

## B.2 Proof of Lemma 2 (See page 10)

Steady states of the system must solve

$$Rp = n_1gp + n_2b,$$

where

$$n_1 = \frac{\exp\{\beta\pi_1\}}{\exp\{\beta\pi_1\} + \exp\{\beta\pi_2\} + \exp\{\beta\pi_3\}}, \quad n_2 = \frac{\exp\{\beta\pi_2\}}{\exp\{\beta\pi_1\} + \exp\{\beta\pi_2\} + \exp\{\beta\pi_3\}},$$

and

$$\pi_1 = (p - Rp)(gp - Rp), \quad \pi_2 = (p - Rp)(b - Rp), \quad \pi_3 = (p - Rp)(-Rp).$$

For  $\beta = 0$  then  $n_1 = n_2 = \frac{1}{3}$ , which implies  $p = \frac{b}{3R-g}$ . The stability of the system can be determined by studying the first order difference equation

$$p_t = \frac{g}{3R}p_{t+1} + \frac{b}{3R},$$

and imposing

$$\left| \frac{dp_t}{p_{t-1}} \right| = \left| \frac{g}{3R} \right| < 1.$$

Since we are working under the assumption that  $g > 0$  and  $R > 1$  the steady state is then locally stable for  $g < 3R$ .

When  $\beta = +\infty$  the price function is piecewise defined as

$$p_t = \begin{cases} \frac{g}{R}p_{t-1} & \text{for } \pi_{1,t-1} > \pi_{2,t-1} \text{ and } \pi_{1,t-1} > \pi_{3,t-1} \\ \frac{b}{R} & \text{for } \pi_{2,t-1} > \pi_{1,t-1} \text{ and } \pi_{2,t-1} > \pi_{3,t-1} \\ 0 & \text{for } \pi_{3,t-1} > \pi_{1,t-1} \text{ and } \pi_{3,t-1} > \pi_{2,t-1} \\ \frac{g}{2R}p_{t-1} & \text{for } \pi_{1,t-1} = \pi_{3,t-1} > \pi_{2,t-1} \\ \frac{b}{2R} & \text{for } \pi_{2,t-1} = \pi_{3,t-1} > \pi_{1,t-1} \\ \frac{g}{3R}p_{t-1} + \frac{b}{3R} & \text{for } \pi_{1,t-1} = \pi_{2,t-1} = \pi_{3,t-1} \end{cases}$$

As before we proceed by analysing the multiple cases:

- (i)  $\pi_{1,t-1} > \pi_{2,t-1}$  and  $\pi_{1,t-1} > \pi_{3,t-1}$ . Then a non-negative steady state  $p$  must

satisfy the following system of equations

$$\begin{cases} p = \frac{g}{R}p \\ (p - Rp)(gp - Rp) > (p - Rp)(b - Rp) \\ (p - Rp)(gp - Rp) > -Rp(p - Rp) \\ p \geq 0 \end{cases}$$

The system however has no solution since the first equation implies either  $p = 0$  or  $g = R$ . In both cases equations two and three are not satisfied as they would hold with equality.

- (ii)  $\pi_{2,t-1} > \pi_{1,t-1}$  and  $\pi_{2,t-1} > \pi_{3,t-1}$ . Then a positive steady state  $p$  must satisfy the following system of equations

$$\begin{cases} p = \frac{b}{R} \\ (p - Rp)(b - Rp) > (p - Rp)(gp - Rp) \\ (p - Rp)(b - Rp) > -Rp(p - Rp) \\ p \geq 0 \end{cases}$$

which has no solution since the third equation is not satisfied for  $b > 0$  and  $p \geq 0$ .

- (iii)  $\pi_{3,t-1} > \pi_{1,t-1}$  and  $\pi_{3,t-1} > \pi_{2,t-1}$ . Then a positive steady state  $p$  must satisfy the following system of equations

$$\begin{cases} p = 0 \\ -Rp(p - Rp) > (p - Rp)(gp - Rp) \\ -Rp(p - Rp) > (p - Rp)(b - Rp) \\ p \geq 0 \end{cases}$$

which has no solution since the second and third equations are not satisfied.

- (iv)  $\pi_{1,t-1} = \pi_{3,t-1} > \pi_{2,t-1}$ . Then a positive steady state  $p$  must satisfy the following system of equations

$$\begin{cases} p = \frac{g}{2R}p \\ -Rp(p - Rp) = (p - Rp)(gp - Rp) \\ -Rp(p - Rp) > (p - Rp)(b - Rp) \\ (p - Rp)(gp - Rp) > (p - Rp)(b - Rp) \\ p \geq 0 \end{cases}$$

which has no solution since the first equation implies either  $p = 0$  which contradicts the third and fourth equation or  $g = 2R$  which contradicts the second equation.

- (v)  $\pi_{2,t-1} = \pi_{3,t-1} > \pi_{1,t-1}$ . Then a non-negative steady state  $p$  must satisfy the follow-



ing system of equations

$$\begin{cases} p = \frac{b}{2R} \\ -Rp(p - Rp) = (p - Rp)(b - Rp) \\ -Rp(p - Rp) > (p - Rp)(gp - Rp) \\ (p - Rp)(b - Rp) > (p - Rp)(gp - Rp) \\ p \geq 0 \end{cases}$$

which has no solution since the first equation contradicts the second.

(vi)  $\pi_{1,t-1} = \pi_{2,t-1} = \pi_{3,t-1}$ . Then a non-negative steady state  $p$  must satisfy the following system of equations

$$\begin{cases} p = \frac{g}{3R}p + \frac{b}{3R} \\ -Rp(p - Rp) = (p - Rp)(b - Rp) \\ -Rp(p - Rp) = (p - Rp)(gp - Rp) \\ (p - Rp)(b - Rp) = (p - Rp)(gp - Rp) \\ p \geq 0 \end{cases}$$

which has no solution since the first equation implies  $p = \frac{b}{3R-g}$  and the second would imply  $b = 0$ .

### B.3 Proof of Lemma 3 (See page 12)

Steady states of the system must solve

$$R\bar{p} = \bar{n}_1 g\bar{p} + \bar{n}_2 b + \bar{n}_3 \bar{p},$$

where

$$\bar{n}_1 = \frac{\exp\{\beta\pi_1\}}{\exp\{\beta\pi_1\} + \exp\{\beta\pi_2\} + \exp\{\beta\pi_3\}}, \quad \bar{n}_2 = \frac{\exp\{\beta\pi_2\}}{\exp\{\beta\pi_1\} + \exp\{\beta\pi_2\} + \exp\{\beta\pi_3\}},$$

and

$$\pi_1 = (\bar{p} - R\bar{p})(g\bar{p} - R\bar{p}), \quad \pi_2 = (\bar{p} - R\bar{p})(b - R\bar{p}), \quad \pi_3 = (\bar{p} - R\bar{p})(\bar{p} - R\bar{p}).$$

For  $\beta = 0$  then  $n_1 = n_2 = \frac{1}{3}$ , which implies  $p = \frac{b}{3R-g-1}$ . The stability of the system can not be directly analysed by the application of dynamical systems theory because of the 'forward looking' element  $p_{t+1}$ .

When  $\beta = +\infty$  the price function is piecewise defined as

$$p_t = \begin{cases} \frac{g}{R}p_{t-1} & \text{for } \pi_{1,t-1} > \pi_{2,t-1} \text{ and } \pi_{1,t-1} > \pi_{3,t-1} \\ \frac{b}{R} & \text{for } \pi_{2,t-1} > \pi_{1,t-1} \text{ and } \pi_{2,t-1} > \pi_{3,t-1} \\ \frac{p_{t+1}}{R} & \text{for } \pi_{3,t-1} > \pi_{1,t-1} \text{ and } \pi_{3,t-1} > \pi_{2,t-1} \\ \frac{g}{2R}p_{t-1} + \frac{p_{t+1}}{2R} & \text{for } \pi_{1,t-1} = \pi_{3,t-1} > \pi_{2,t-1} \\ \frac{b}{2R} + \frac{p_{t+1}}{2R} & \text{for } \pi_{2,t-1} = \pi_{3,t-1} > \pi_{1,t-1} \\ \frac{g}{3R}p_{t-1} + \frac{b}{3R} + \frac{p_{t+1}}{3R} & \text{for } \pi_{1,t-1} = \pi_{2,t-1} = \pi_{3,t-1} \end{cases}$$

As before we proceed by analysing the multiple cases:

- (i)  $\pi_{1,t-1} > \pi_{2,t-1}$  and  $\pi_{1,t-1} > \pi_{3,t-1}$ . Then a non-negative steady state  $p$  must satisfy the following system of equations

$$\begin{cases} p = \frac{g}{R}p \\ (p - Rp)(gp - Rp) > (p - Rp)(b - Rp) \\ (p - Rp)(gp - Rp) > (p - Rp)(p - Rp) \\ p \geq 0 \end{cases}$$

The system however has no solution since the first equation implies either  $p = 0$  or  $g = R$ . In both cases equations two and three are not satisfied as they would hold with equality.

- (ii)  $\pi_{2,t-1} > \pi_{1,t-1}$  and  $\pi_{2,t-1} > \pi_{3,t-1}$ . Then a non-negative steady state  $p$  must satisfy the following system of equations

$$\begin{cases} p = \frac{b}{R} \\ (p - Rp)(b - Rp) > (p - Rp)(gp - Rp) \\ (p - Rp)(b - Rp) > (p - Rp)(p - Rp) \\ p \geq 0 \end{cases}$$

which has no solution since the third equation is not satisfied for  $b > 0$  and  $p \geq 0$ .

- (iii)  $\pi_{3,t-1} > \pi_{1,t-1}$  and  $\pi_{3,t-1} > \pi_{2,t-1}$ . Then a non-negative steady state  $p$  must satisfy the following system of equations

$$\begin{cases} p = \frac{p}{R} \\ (p - Rp)(p - Rp) > (p - Rp)(gp - Rp) \\ (p - Rp)(p - Rp) > (p - Rp)(b - Rp) \\ p \geq 0 \end{cases}$$

which has no solution since the first equation implies either  $p = 0$  or  $R = 1$ .

- (iv)  $\pi_{1,t-1} = \pi_{3,t-1} > \pi_{2,t-1}$ . Then a non-negative steady state  $p$  must satisfy the follow-

ing system of equations

$$\begin{cases} p = \frac{g}{2R}p + \frac{p}{2R} \\ (p - Rp)(p - Rp) = (p - Rp)(gp - Rp) \\ (p - Rp)(p - Rp) > (p - Rp)(b - Rp) \\ (p - Rp)(gp - Rp) > (p - Rp)(b - Rp) \\ p \geq 0 \end{cases}$$

which has no solution since the first equations imply either  $p = 0$  which contradicts the third and fourth equation or  $g = 2R - 1$  which contradicts the second equation that implies  $g = R$ .

- (v)  $\pi_{2,t-1} = \pi_{3,t-1} > \pi_{1,t-1}$ . Then a positive steady state  $p$  must satisfy the following system of equations

$$\begin{cases} p = \frac{b}{2R} + \frac{p}{2R} \\ (p - Rp)(p - Rp) = (p - Rp)(b - Rp) \\ (p - Rp)(p - Rp) > (p - Rp)(gp - Rp) \\ (p - Rp)(b - Rp) > (p - Rp)(gp - Rp) \\ p \geq 0 \end{cases}$$

which has no solution since the first equation implies  $p = \frac{b}{2R-1}$  and the second  $p = b$  which is possible only for  $R = 1$ .

- (vi)  $\pi_{1,t-1} = \pi_{2,t-1} = \pi_{3,t-1}$ . Then a positive steady state  $p$  must satisfy the following system of equations

$$\begin{cases} p = \frac{g}{3R}p + \frac{b}{3R} + \frac{p}{3R} \\ (p - Rp)(p - Rp) = (p - Rp)(b - Rp) \\ (p - Rp)(p - Rp) = (p - Rp)(gp - Rp) \\ (p - Rp)(b - Rp) = (p - Rp)(gp - Rp) \\ p \geq 0 \end{cases}$$

which has no solution since equations two to four imply either  $p = 0$  which contradicts equation one or  $p = b = gp$  implying  $g = 1$ . Then the first equation would read  $3Rb = 3b$  which implies  $R = 1$ .

#### B.4 Eigenvalues for the two type model

It is convenient to rewrite the model in (8) and (9) transforming it from a univariate third order difference equation to a first order difference equation with three states. We use the following change of variables  $(p_t, p_{t-1}, p_{t-2}) = (x_{t+1}, w_{t+1}, z_{t+1})$  to rewrite the model as the following system:

$$\begin{cases} x_{t+1} = \frac{g}{R}x_t \{1 + \exp[\beta(x_t - R w_t)(b - g z_t)]\}^{-1} + \frac{b}{R} \left(1 - \{1 + \exp[\beta(x_t - R w_t)(b - g z_t)]\}^{-1}\right) \\ w_{t+1} = x_t \\ z_{t+1} = w_t \end{cases}$$

Taking first order derivatives we get the following Jacobian matrix

$$\begin{bmatrix} A & B & C \\ 1 & 0 & 0 \\ 0 & 1 & 0 \end{bmatrix},$$

with

$$A = \frac{((\beta g^2 z_t - b\beta g) x_t - b\beta g z_t + g + b^2\beta) e^{\beta \cdot (b - g z_t)(x_t - R w_t)} + g}{R \cdot (e^{\beta \cdot (b - g z_t)(x_t - R w_t)} + 1)^2},$$

$$B = -\frac{\beta \cdot (g x_t - b) (g z_t - b) e^{\beta \cdot (b - g z_t)(x_t - R w_t)}}{(e^{\beta \cdot (b - g z_t)(x_t - R w_t)} + 1)^2},$$

$$C = \frac{\beta g \cdot (x_t - R w_t) (g x_t - b) e^{\beta \cdot (x_t - R w_t)(b - g z_t)}}{R \cdot (e^{\beta \cdot (x_t - R w_t)(b - g z_t)} + 1)^2}.$$

To evaluate the stability of the steady state, one can observe the eigenvalues of the Jacobian matrix, which in this case are given by:

$$\lambda_1 = \frac{\sqrt[3]{2A^3 + 3\sqrt{3}\sqrt{4A^3C - A^2B^2 + 18ABC - 4B^3 + 27C^2} + 9AB + 27C}}{3\sqrt[3]{2}} - \frac{\sqrt[3]{2}(-A^2 - 3B)}{3\sqrt[3]{2A^3 + 3\sqrt{3}\sqrt{4A^3C - A^2B^2 + 18ABC - 4B^3 + 27C^2} + 9AB + 27C}} + \frac{A}{3}$$

$$\lambda_2 = -\frac{1}{6\sqrt[3]{2}}(1 - i\sqrt{3})\sqrt[3]{2A^3 + 3\sqrt{3}\sqrt{4A^3C - A^2B^2 + 18ABC - 4B^3 + 27C^2} + 9AB + 27C} + \frac{(1 + i\sqrt{3})(-A^2 - 3B)}{3 \cdot 2^{2/3}\sqrt[3]{2A^3 + 3\sqrt{3}\sqrt{4A^3C - A^2B^2 + 18ABC - 4B^3 + 27C^2} + 9AB + 27C}} + \frac{A}{3}$$

$$\lambda_3 = -\frac{1}{6\sqrt[3]{2}}(1 + i\sqrt{3})\sqrt[3]{2A^3 + 3\sqrt{3}\sqrt{4A^3C - A^2B^2 + 18ABC - 4B^3 + 27C^2} + 9AB + 27C} + \frac{(1 - i\sqrt{3})(-A^2 - 3B)}{3 \cdot 2^{2/3}\sqrt[3]{2A^3 + 3\sqrt{3}\sqrt{4A^3C - A^2B^2 + 18ABC - 4B^3 + 27C^2} + 9AB + 27C}} + \frac{A}{3}$$

## B.5 Eigenvalues for the model with fundamentalist

As before we rewrite the model as the “following” system:

$$\begin{cases} x_{t+1} = \frac{g}{R}x_t n_{1,t} + \frac{b}{R}n_{2,t} \\ w_{t+1} = x_t \\ z_{t+1} = w_t \end{cases}$$

with

$$n_{1,t} = \frac{\exp[\beta(x_t - R w_t)(g z_t - R w_t)]}{Z_t},$$

$$n_{2,t} = \frac{\exp[\beta(x_t - R w_t)(b y_{t-3} - R w_t)]}{Z_t},$$

$$n_{3,t} = \frac{\exp[\beta(x_t - R w_t)(-R w_t)]}{Z_t},$$

$$Z_t = \exp[\beta(x_t - R w_t)(g z_t - R w_t)] + \exp[\beta(x_t - R w_t)(b y_{t-3} - R w_t)] + \exp[\beta(x_t - R w_t)(-R w_t)].$$

Taking first order derivatives we get the following Jacobian matrix:

$$\begin{bmatrix} A & B & C \\ 1 & 0 & 0 \\ 0 & 1 & 0 \end{bmatrix}$$

$$A = \frac{e^{R\beta w \cdot (x - R w)} \cdot (g e^{2\beta \cdot (g z - R w)(x - R w) + R\beta w \cdot (x - R w)} + e^{\beta \cdot (g z - R w)(x - R w)} \cdot (((\beta g^2 z - b\beta g) x - b\beta g z + g + b^2\beta) e^{\beta \cdot (b - R w)(x - R w) + R\beta w \cdot (x - R w)} + \beta g^2 z x + g) + b^2\beta e^{\beta \cdot (b - R w)(x - R w)})}{R \cdot (e^{\beta \cdot (g z - R w)(x - R w) + R\beta w \cdot (x - R w)} + e^{\beta \cdot (b - R w)(x - R w) + R\beta w \cdot (x - R w)} + 1)^2},$$

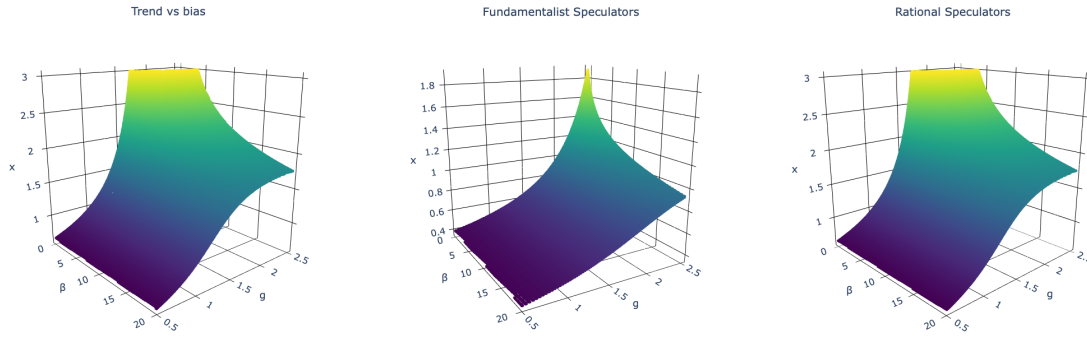
$$B = -\frac{\beta e^{R\beta w \cdot (x - R w)} \cdot (e^{\beta \cdot (x - R w)(g z - R w)} \cdot (((g^2 x - b g) z - b g x + b^2) e^{\beta \cdot (b - R w)(x - R w) + R\beta w \cdot (x - R w)} + g^2 x z) + b^2 e^{\beta \cdot (b - R w)(x - R w)})}{(e^{\beta \cdot (x - R w)(g z - R w) + R\beta w \cdot (x - R w)} + e^{\beta \cdot (b - R w)(x - R w) + R\beta w \cdot (x - R w)} + 1)^2},$$

$$C = \frac{\beta g \cdot (x - R w) \cdot ((g x - b) e^{\beta \cdot (b - R w)(x - R w) + R\beta w \cdot (x - R w)} + g x) e^{\beta \cdot (x - R w)(g z - R w) + R\beta w \cdot (x - R w)}}{R \cdot (e^{\beta \cdot (x - R w)(g z - R w) + R\beta w \cdot (x - R w)} + e^{\beta \cdot (b - R w)(x - R w) + R\beta w \cdot (x - R w)} + 1)^2}.$$

The general form of the eigenvalues computed in section (B.4) is still valid, so that we can obtain them by simply replacing the formulae for  $A$ ,  $B$  and  $C$ .

## C Steady States

In the figure below we numerically solve for the implicit function defining the steady state of the systems. To obtain a plot in three dimension we fix the value of the parameters  $R = 1.01$  and  $b = 1$  and vary the parameters  $g$  and  $\beta$ .



## D Numerical errors for the EP method

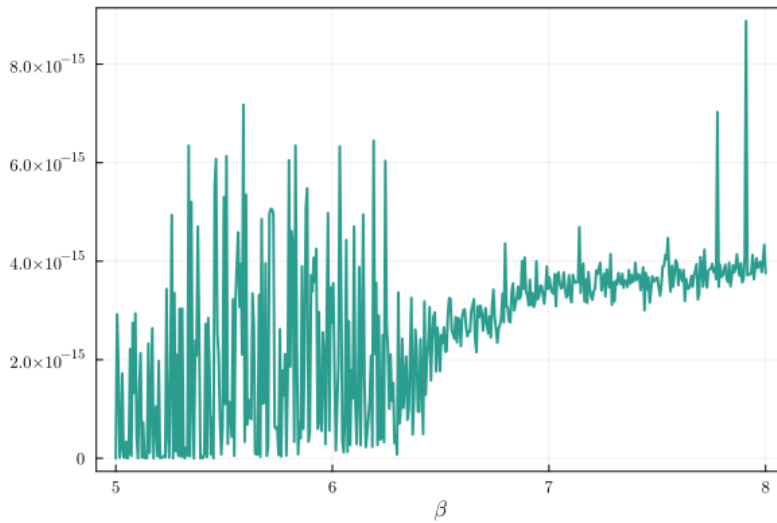


Figure 12: Sum of absolute errors

## E Neural Network

The network architecture we use is the following.

Hidden Layers	Hidden Layer size	Activation	Loss	Optimizer	epochs
1	16	tanh	mse	adam	1000

An overview of the Neural Network is given below, while we refer to [Goodfellow, Bengio and Courville \(2016\)](#) for full details on this kind of models.

**Input Layer** The input layer passes the input data to the next layer. Denote the input as  $\mathbf{X} \in \mathbb{R}^k$ , where  $k$  is the size of the input vector.

**Hidden Layer** The first dense layer transforms the input  $\mathbf{X}$  using a weight matrix  $\mathbf{W}_1 \in \mathbb{R}^{k \times 16}$ , a bias vector  $\mathbf{b}_1 \in \mathbb{R}^{16}$ , and applies the tanh activation function. The operation can be described by the equation:

$$\mathbf{H} = \tanh(\mathbf{W}_1^\top \mathbf{X} + \mathbf{b}_1)$$

Here,  $\mathbf{H} \in \mathbb{R}^{16}$  is the output of the hidden layer, which becomes the input to the next layer.

**Output Layer** The output layer further transforms the output of the hidden layer  $\mathbf{H}$  using another weight matrix  $\mathbf{W}_2 \in \mathbb{R}^{16 \times 1}$ , a bias term  $b_2 \in \mathbb{R}$ , and applies a linear activation function. The operation for the output layer is given by:

$$\mathbf{Y} = \mathbf{W}_2^T \mathbf{H} + b_2$$

$\mathbf{Y} \in \mathbb{R}$  is the scalar output of the network, that approximates the state variable. The input vector in section (4) is of size  $k$  and contains  $p_{t-1}, p_{t-2}$  and  $p_{t-3}$  while the target is  $p_{t+1}$ . In section (5) the size is equal to 9 and the input vector contains  $x_{t-1}, x_{t-2}, x_{t-3}, w_{t-1}, w_{t-2}, w_{t-3}, R_t, R_{t-1}, R_{t-2}$ , that is lags of the Bitcoin in deviation form, of the BiTSI index and of the time varying risk-free rate.

## F Stationarity tests

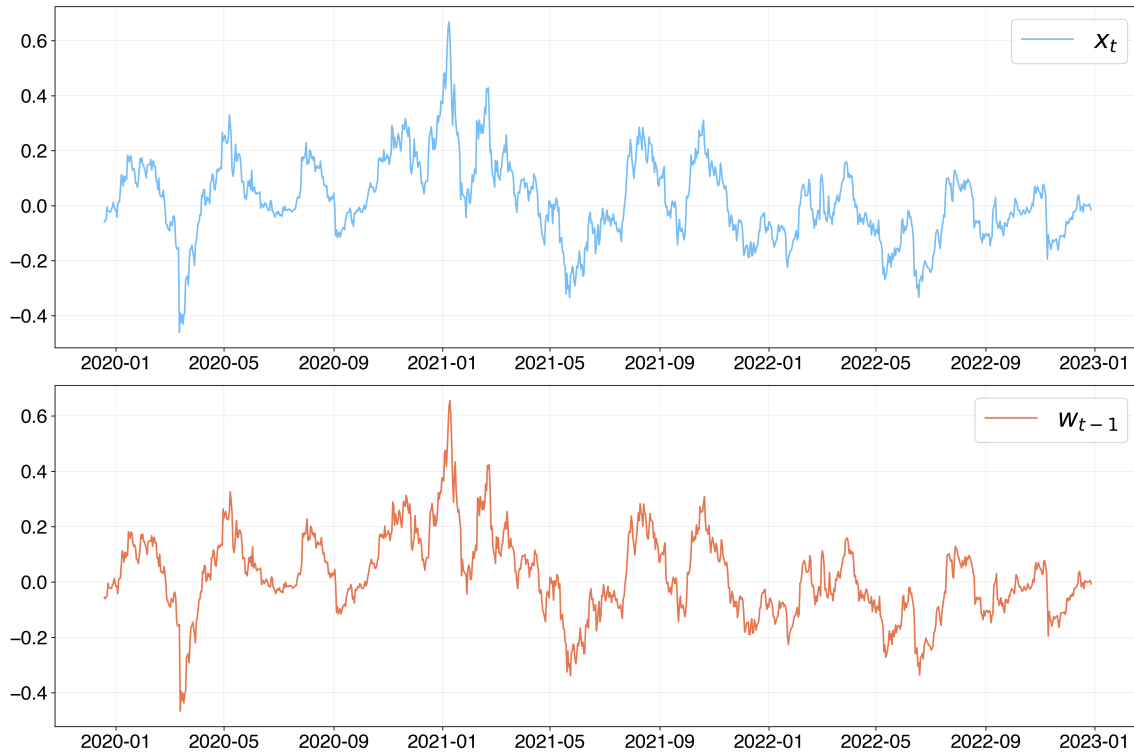


Figure 13: Variable for the estimation

We test the presence of a unit root for the two time series related to the percentage deviation form the moving average fundamental by means of the augmented Dickey–Fuller test (ADF). The associated p-values are:  $1.27e-06$  for  $x_t$  and  $0.037$  for  $w_{t-1}$ . We can therefore reject the null hypothesis of unit root of the ADF.

## G Robustness to different windows

In this section we check the robustness of the estimation to a different choice of the window length in the moving average fundamental value. We repeat the analysis for each value between 1 and 99. A window choice of 1 implies that we are actually estimating the model on daily returns. For each choice we re estimate the two types model with trend followers and bias and plot the point estimate of the parameters with associated standard errors in the top panel of Figure 14, the dashed line is at 0. The bottom panel shows the p-value for the F-statistic of significance of the non-linear model with respect to the linear one and the adjusted r-squared. The dashed line marks the 5% significance level.

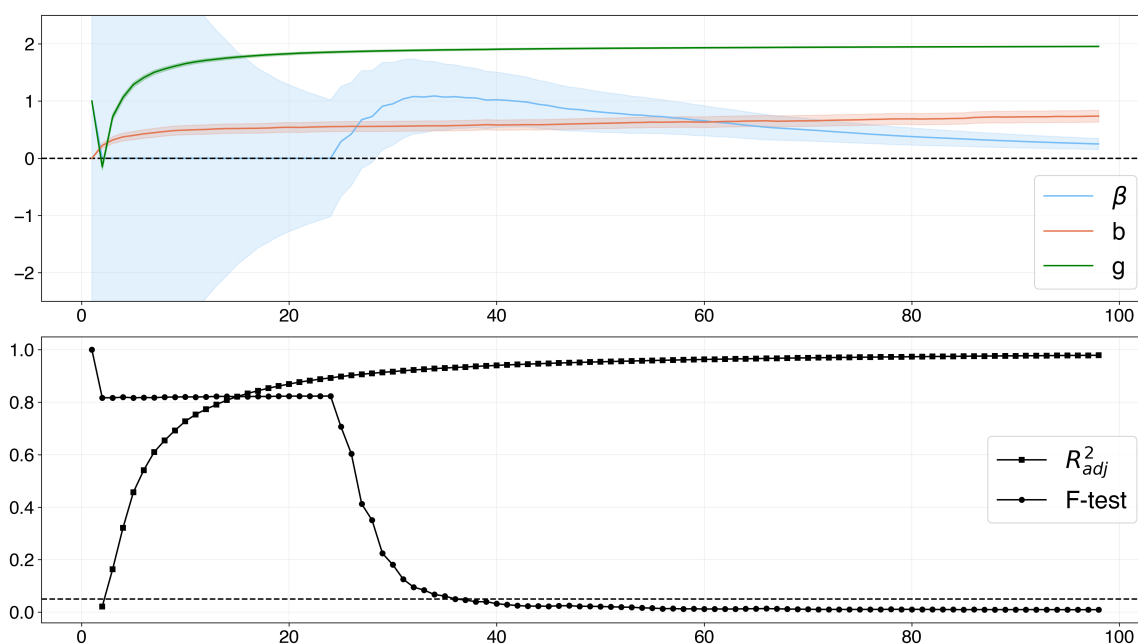


Figure 14: Effect of different windows

Daily returns (window length = 1) are as one would expect unpredictable, with an adjusted r-squared close to 0. For a window length smaller than 25 the intensity of choice  $\beta$  is not significantly different from 0, For values lower than 7 we get estimates ranging so much that we had to impose limits on the axis in order to obtain a meaningful visualization. For values higher than 30 however we start to observe results that are quantitatively similar with high R-squared, positive and significant  $\beta$ s and preference for the non-linear model as conveyed by the p-value of the F-test.

## H Bootstrapped standard errors

In this section we show the robustness of the standard errors by computing them via bootstrap. The p-value of the test for Conditional Heteroscedasticity does not reject homoskedasticity in the residuals. Nonetheless we follow the approach of [Goncalves and Kilian \(2004\)](#). That is for 2000 bootstrap replications we generate a series of pseudo resid-



uals by multiplying the original residuals by a random number drawn from a Standard Normal Distribution We then create a pseudo time series using the associated non-linear model by replacing the actual residuals with the pseudo residuals. Finally we re-estimate the model using the pseudo time series to obtain a new set of parameter estimates and report the values of the associated confidence interval at the .99 percent level in Table 4.

Table 4: 99% bootstrapped confidence intervals

	g	b	$\beta$
<i>Trend chasers vs pure bias:</i>	[1.87 1.94]	[0.41 0.76]	[0.03 2.01]
<i>Tc vs B vs Fundamentalist:</i>	[2.81 2.9]	[0.61 1.14]	[0.03 1.0]
<i>Tc vs B vs Rational Expectations:</i>	[1.87 1.96]	[0.58 1.1]	[0.12 2.85]